Detection of hydroperoxy complex in the oxidative reactions of myoglobin with hydrogen peroxide

by

Héctor D. Arbelo-López

A thesis submitted in partial fulfillment of the requirements for the degree of

MASTER OF SCIENCE
In
Chemistry

UNIVERSITY OF PUERTO RICO
MAYAGÜEZ CAMPUS
2008

Approved by:

_____	_____
Marisol Vera-Colón, PhD Member, Graduate Committee	Date
_____	_____
Mayra E. Cádiz-García, PhD Member, Graduate Committee	Date
_____	_____
Juan López-Garriga, PhD President, Graduate Committee	Date
_____	_____
Arturo Hernández-Maldonado, PhD Representative of Graduate Studies	Date
_____	_____
Francis Patron, PhD Chairperson of the Department	Date

ABSTRACT

A large number of heme enzymes catalyze the heterolysis of hydrogen peroxide (H_2O_2) and H_2O_2 is used as a source of oxidizing equivalents for biological oxidative reaction. Despite the increased understanding of the reactions of heme with H_2O_2, the heme-hydroperoxy complex has never been identified at ambient temperature. To gain insight into this problem, we adapted laser flash photolysis spectroscopy with a stopped-flow rapid mixing device. This technique was used to probe the kinetic behavior of myoglobin with carbon monoxide in the presence of hydrogen peroxide, in the nano to microseconds timescale. Our results show for the first time that after photolysis a reaction intermediate, possibly the heme-hydroperoxide complex, is present at 426 nm, subsequently this intermediate species gives rise to the compound II species at 418 nm, respectively. The data allows suggesting a model where hydrogen peroxide binds to deoxyMb and forms the hydroperoxy species which give rise to the compound II species.

RESUMEN

Una gran cantidad de hemo proteínas enzimas catalizan la reaccion del peróxido de hidrógeno (H_2O_2) y utilizan H_2O_2 como fuente oxidante para reacciónes biológica. A pesar del entendimiento adquirido, la completa dilucidación de las reacciones de hemo proteínas con el peróxido de hidrógeno está lejos de estar completa. Entre los intermediarios que todavia no se conocen está el complejo de hemo-hidroperóxido el cual nunca se ha podido identificar a temperatura ambiente. Para obtener mayor conocimiento de este problema hemos adaptado la técnica de fotólisis por destello de láser con un dispositivo de mezcla rápida de flujo detenido. Esta técnica fue utilizada para sondear el comportamiento cinético de mioglobina (Mb) con monóxido de carbono en presencia de peróxido de hidrógeno, en la escala de nano a micro segundos. Nuestros resultados demuestran por primera vez que después de la fotodescomposición que un precursor del compuesto I está evidenciado por una banda a 426 nm, esta especie transitoria genera posteriormente la especie de compuesto II con banda en 418 nm. Los datos permiten sugerir un modelo en donde el peróxido de hidrógeno se enlaza a deoxyMb generando la especie de hidroperóxido que a su vez genera la especie de compuesto II.

To GOD, my family and friends . . .

"There are men who struggle for a day and they are good.
There are men who struggle for a year and they are better.
There are men who struggle many years, and they are better still.
But there are those who struggle all their lives:
These are the indispensable ones."
Bertolt Brecht

ACKNOWLEDGEMENTS

During my graduate school years at the University of Puerto Rico, several persons and institutions collaborated directly and indirectly with my research. Without their support it would be impossible for me to finish my work. That is why I wish to dedicate this section to recognize their support.

I want to start expressing a sincere acknowledgment to the Grants from NSF and NIH that provided the funding and the resources for the development of this research; and to my advisor, Dr. Juan López Garriga because he gave me the opportunity to carry out research under his guidance and supervision. I received motivation; encouragement and support from him during all my studies. I also want to thank the example, motivation, inspiration and support, first to GOD who was with me during the darkest hour and showed me that it can't rain all the time. To my wife Mical who has been my fiercest supporter all this time. To my nieces Zrayre and Zoery whom with their inconditional love gave me inspiration for this project. At last, but not less important, I would like to thank my family, and friends Gardy, Elddie, Maria, Anthony, Neit, Edra, Waldy and Joel for always believing in me and for supporting me.

TABLE OF CONTENTS

TABLE OF TABLES

Tables **Page**

TABLE OF FIGURES

Figures **Page**

1. INTRODUCTION

1.1 Hydrogen peroxide and Peroxidases

Hydrogen peroxide (H_2O_2) is a light blue liquid that is colorless in aqueous solution. Hydrogen peroxide is a weak acid and therefore one of the strongest oxidizers known. It can corrode many materials and burn human skin. Hydrogen peroxide decomposes to water and oxygen by a two electron reduction spontaneously following the next equation:

$$H_2O_2 \rightarrow 2\ H_2O + O_2 \quad \textbf{(1)}$$

The hydrogen peroxide decomposition reaction is thermodynamically favorable at room conditions. This reaction has a $\Delta H°$ of $-99\ kJ \cdot mol^{-1}$. The decomposition reaction has redox potential versus a normal hydrogen electrode at 25°C and at pH 7 of 1.77 V. The rate of the reaction is dependent of temperature, concentration and pH. However, the hydrogen peroxide molecule has a long life because the peroxide (O-O) bond is relatively strong. The O-O bond distance in the hydrogen peroxide molecule is approximately 1.47 Å and has bond energy of 51 $kcal*mol^{-1}$ (Cotton et al., 1999). With this strong O-O bond, in order to facilitate the break up of H_2O_2 into water and oxygen, it is necessary to cleave the peroxide bond. This bond cleavage unleashes the oxidizing power of hydrogen peroxide. Hydrogen peroxide decomposition has dangerous side effects because of the generation of highly unstable and reactive oxidizing agents like superoxide (O_2^-) and hydroxyl radical ($OH^{\cdot}$). The reactivity of hydrogen peroxide and those oxidizing agents can cause severe damage to macromolecules in biological systems. Hydrogen peroxide is naturally generated as a byproduct of cellular oxygen metabolism, oxidative stress and other reactive oxygen species

that damage the DNA, proteins and cell membranes. Mechanisms for coping with oxidative stress are crucial for the survival of all organisms (Seib et al., 2006).

As a result of the dangerous oxidizing effects of hydrogen peroxide and the potential damages it causes to biological systems, nature has found a way to provide a mechanism to solve this problem. This defense mechanism against oxidative stress is through a family of enzymes that catalyze hydrogen peroxide harmlessly, called peroxidases. Peroxidases not only decompose hydrogen peroxide, but capable of taking advantage of its oxidizing power to catalyze a number of oxidative reactions. Peroxidases are found in plants, bacteria and animals and form an enzyme super family. Figure 1.1 shows all different classes of heme peroxidases. Some examples of different members of the peroxidase family are going to be briefly mentioned ahead. One of these members is the haloperoxidase family. Haloperoxidases catalyze the halides transformation in the presence of hydrogen peroxide. Haloperoxidases can halogenate a broad range of organic compounds. Haloperoxidases are found in fungi, bacteria and red algae. One example of a haloperoxidase is chloroperoxidase. Chloroperoxidase is a heme containing glycoprotein which catalyzes halogenations reactions using hydrogen peroxide. This enzyme has unique aspects, but has a distal polar pocket commonly found in other Peroxidases (Kühnel et al., 2006). Chloroperoxidase exhibits peroxidase, catalase and cytochrome P450 activity as well to catalyzing halogenation reactivity. Another example is peroxidase-cyclooxygenase. Members of this family reduce hydrogen peroxide and oxidize a variety of organic and inorganic compounds. Some representatives of this family are: Myeloperoxidase, Lacto peroxidase, Eosinophil peroxidase, and Thyroid peroxidase. The myeloperoxidase consists of two 15 kDa light

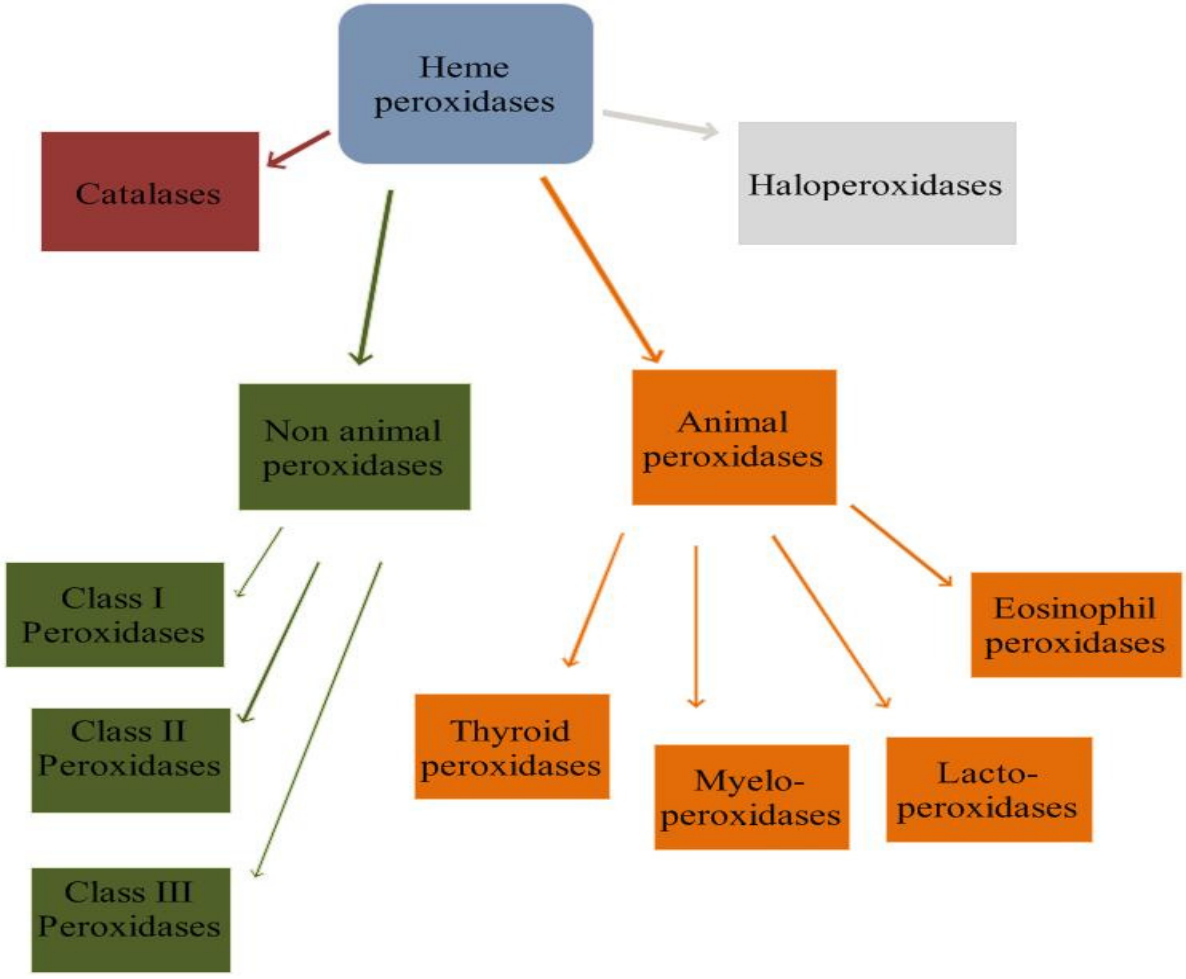

Figure 1.1 All different classes of heme peroxidases. Some of the family members previously mentioned are: haloperoxidases, non-animal peroxidases and catalases.

chains and two glycosylated heavy chains bound to a heme group. Myeloperoxidase in great quantities is present in neutrophils which are the most common type of white blood cells in humans. Myeloperoxidases uses H_2O_2 and chloride anion to produce Hypochlorous acid and tyrosyl radical which are used to kill bacteria. Eosinophil peroxidase similar to myeloperoxidase is involve in combating infections and parasites and is present in another type of white cell called Eosinophil granulocytes (van Dalen and Kettle, 2001). Lactoperoxidase is a single peptide chain glycoprotein present in milk. It has antioxidant and antimicrobial properties. Lactoperoxidase uses H_2O_2 to oxydate thiocyanate ions (SCN^-) producing hypothiocyanate ($OSCN^-$) which is considered to be bactericidal. Thyroid peroxidase is expressed in the thyroid as responsible of thyroids hormone biosynthesis.

Another important member of the peroxidase family is the catalases. Catalases are bifunctional antioxidant enzymes present in different organisms. Almost all known organisms have catalases in every organ, and it is normally found in high concentrations in the liver. Catalases provide protection against oxidative stress by converting two hydrogen peroxide molecules into water and oxygen. One example of the use of catalase by nature is in the use as a propellant generator used by the bombardier beetle. The bombardier beetle has two sets of chemicals ordinarily stored separately in its paired glands. The largest of the pair of storage reservoir contains hydroquinones and hydrogen peroxide, whereas the smallest of pair of the chambers contains catalases. To activate the spray, the beetle mixes the contents of the two compartments, causing oxygen to be liberated from hydrogen peroxide decomposition. The oxygen liberated oxydizes the hydroquinones and also acts as a propellant. The structures found of catalase have revealed an unusually large number of

modifications unique to catalases. These modifications are a result of the interaction with reactive oxygen species. Biochemical and physiological characterization of catalases from many different organisms has revealed a surprisingly wide range of catalytic efficiencies, despite similar sequences (Chelikani et al., 2005). These enzymes are very stable and are more resistant to pH, temperature and proteolysis than other enzymes. This is attributed to a very rigid structure that is resistant to unfolding structure.

The last group of peroxidases is the non-animal peroxidases group which it is divided in three major classes. The first class (Class I) of peroxidases is a group of intracellular peroxidases. Three members of this class are: yeast cytochrome c peroxidase found in the mitochondria, which serve as a protection mechanism for peroxides; ascorbate peroxidase, which is the main protection and removes hydrogen peroxidase in the chloroplast and cytoplasm in plants, and bacterial catalase which is responsible for protection of cells under oxidative stress and exhibit both peroxidase and catalase activities. Cytrochrome C peroxidase is an example of a heme containing oxidoreductase that catalyzes a two-electron reduction of hydrogen peroxide to water with concomitant oxidation of two equivalents of cytochrome C. Phylogenetic analysis has demonstrated that it is obvious that a large diversity in the genes coding for CcPs occurs among fungal genomes. The natural expression of the putative CcP genes from all three subfamilies of CcP is a response to various forms of oxidative stress in the fungal life cycle (Zamocky and Dunand, 2006). The second class (Class II) of peroxidases is composed of secretorial fungal peroxidases. This class has four conserved disulfide bridges and two calcium binding site. One member of this class is lignin peroxidases that are monomeric glycoproteins involved in lignin degradation. Lignin

peroxidase catalyzes the H_20_2-dependent oxidation of a variety of lignin model compounds. Lignin is the most abundant aromatic polymer on earth. It comprises 15 to 30% of woody plant cell walls, forming a matrix surrounding the cellulose that significantly retards the microbial degradation of cellulose and hence lignin plays a key role in the earth's carbon cycle. When it is compared to CcP, its heme pocket opening is smaller than in CcP which can explain the differences in reactivity of the two hemes. This same opening may provide the site for binding small aromatic substrates. Lignin peroxidase has a carboxylate-carboxylate hydrogen bond important for heme binding that is not present in cytochrome c peroxidase. And finally, lignin peroxidase contains 2 structural calcium ions while cytochrome c peroxidase contains no calcium ions (Poulos et al., 1993). The third class (Class III) has multiple tissue specific functions and is only found in plants. This class of proteins is monomeric glycoproteins that contain, as Class II, four conserved disulfide bridges and calcium ions but the disulfides bridges location differ from Class II enzymes. Class III peroxidases participate in many different plant processes.

Peroxidases come from various organisms and have a very important biological role in nature. When these enzymes are structurally compared with each other some have very similar amino acid sequences but others are different in their amino acid sequences resulting in a low percent of primary sequence homology. However, all have in common a highly conserved tertiary structure. This pattern, where the tertiary structure is more conserved than primary structure, is rather widespread in many families of enzymes. This structural similarity of heme peroxidases is reflected around the common 10 helical bundle motifs. All peroxidases are heme containing enzymes. Figure 1.2 shows the active site of horseradish

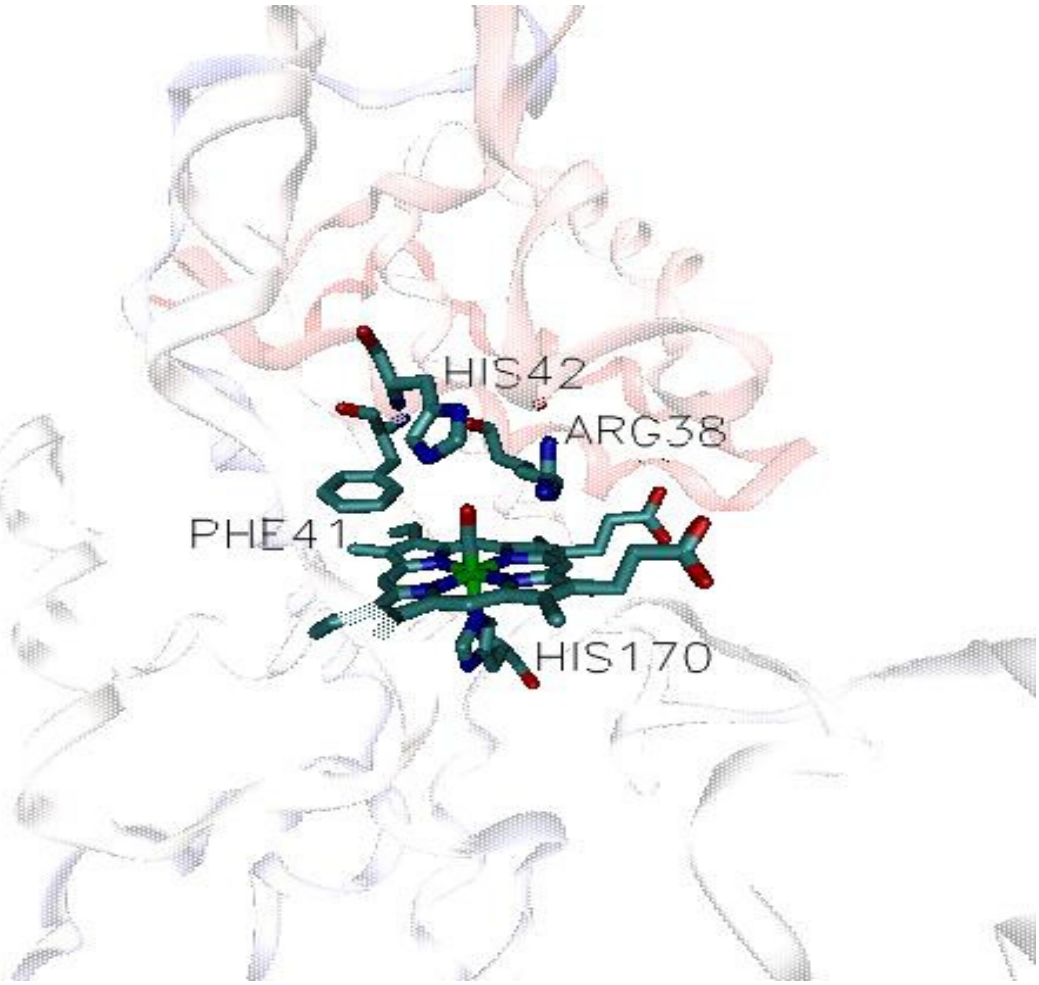

Figure 1.2 Horseradish peroxidase active site from 1W4Y pdb with His170 in the proximal position and His 42, Arg 38, Phe 41 as the distal amino acids (Carlsson et al., 2005).

peroxidase (HRP). In its active site the His 170 is coordinated to the heme iron attaching the heme group to the protein matrix. In the distal side of the pocket we have the His 42, Arg 38 and Phe 41 (Carlsson et al., 2005). It is attributed to the distal amino acids which are directly involved in the reaction of peroxidases with hydrogen peroxide. The distal amino acids interact with the different intermediates of the peroxidase reaction. Similar to hemoglobin and myoglobin, peroxidases have, as a prosthetic group, a large organic heterocyclic named protoporphyrin IX. This large organic heterocyclic is composed of four pyrroline subunits interconnected via their α carbon atoms via methine bridges (=CH-). It has a coordinated iron to the four nitrogen atoms of the pyrroline subunits. Figure 1.3 shows the protoporphyrin IX group. The iron has the fifth and sixth coordination positions free. One of the free coordination positions is used by a covalent bond to an active site enzyme amino acid which attaches the heme group to the protein matrix. All peroxidases have a distal and proximal helix loop close to the heme group. The proximal helix contains a His which is coordinated to the fifth coordination position of the iron in the heme group. This is conserved through most peroxidase and hemoglobins excluding catalases that provide an example of heme proteins where a proximal Tyr residue coordinates to the heme iron.

The proposed mechanism of the reaction of hydrogen peroxide with peroxidases is shared with other heme proteins like super oxide dismuthase, cytochrome p450 and myoglobin. The most accepted mechanism proposed is an acid –base process in which the distal His is involved in this process (Poulos and Kraut, 1980). For a classic peroxidase, such as HRP, the reaction cycle involves a two-electron oxidation-reduction. (Hersleth et al., 2007) Previous studies have demonstrated that myoglobin reacts in a similar fashion with

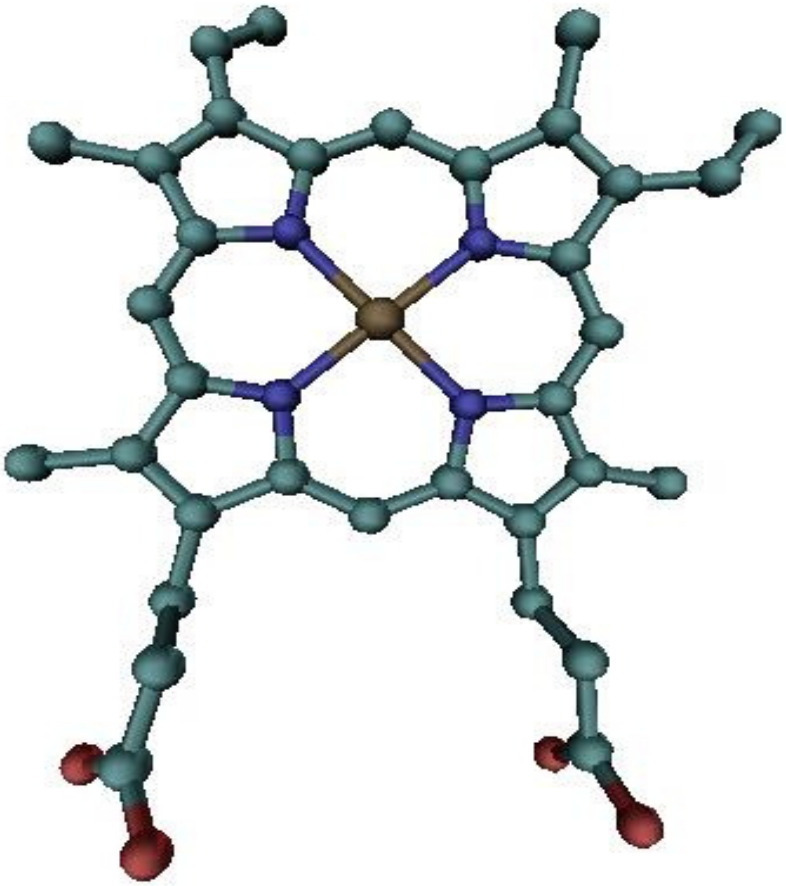

Figure 1.3 Protoporphyrin IX heme group. The red spheres are the oxygen atoms of the propionates and the blue spheres are the nitrogens atoms of the pyrrolines and in brown we have the iron atom.

hydrogen peroxidase to give a ferryl species, meaning that myoglobin is useful as a model to give insight in this reaction. Further explanation of this mechanism will be addressed in the next sections.

1.2 Myoglobin background and structure

Myoglobin is a small monomeric globular protein of 153 amino acids. Myoglobin is part of the globin super family that is well studied and widely distributed through wide variety organisms (Vinogradov et al., 2006). The globins family of proteins takes parts in very import biological processes that are diverse, and metabolize important physiological reactions vital to life of most organisms from protist to mammals. (Prasad and Mitra, 2004) Some of the known functions are the transport of diatomic molecules, chemical catalysis, and electron transfer. Phylogenetic analysis of the globin family suggests that all globins have evolved from a common ancestor. It is found through phylogenetic analysis that globins are mostly enzymes, and that the transport of oxygen is a function that was developed relatively recently through the emergence of multicellular organisms (Vinogradov et.al., 2006).

Myoglobin is primary responsible for oxygen transport in muscle. (Ordway and Garry, 2004) Myoglobin is frequently found in muscle cells and gives meat its typical red color. Figure 1.4 shows the structure of horse heart met-myoglobin. Over 80% of the polypeptide chain is involved in eight helical segments (Evans and Brayer, 1990). Its protein matrix is composed of eight (8) helical motifs compared to ten (10) found in peroxidases. Myoglobins similar to peroxidases have a heme group in their active site. The free heme group binds CO more strongly than oxygen, but Mb is capable of discriminating between both. Two explanations have been proposed for this behavior. One, is an unfavorable CO binding

because it is forced to be in a bent configuration. And the second one is that oxygen is stabilized by hydrogen bonding with the distal His.

Regarding this, a significant and important number of research contributions have clearly presented the relation between the Mb structure and its relation to ligand selection, affinity, and dynamics. Furthermore, the role of Mb heme pocket amino acids and its contribution to electrostatic effects, steric constraints, hydrogen-bonding differences, and proximal *trans* effect has also been deeply discussed. For example, it has been suggested that equilibrium and kinetic data should be obtained for carbon monoxide binding to Mb and several single mutants (i.e. His64 to Ala, Val, Leu, and Gln and Val 68 to Ala and Asn) before the relative stability of mutants can be meaningfully compared (Chatfield et al., 1987). Similarly, His 64 was substituted for Gly, Val, Phe, Cys, Met, Lys, Arg, Asp, Thr and Tyr to address the discrimination between oxygen and carbon monoxide. These substitutions altered O_2 and CO affinities and indicated that His64 discriminates between O_2 and CO binding by sterically hindering bound CO and stabilizing O_2 through hydrogen bonding (Johnson, 1970). The X-ray structures of metMb with hydrophobic substitutions at residue 64 (Val64 and Leu64) showed to lack a water molecule at the sixth coordination position, while those with polar amino acids (i.e. His64 and Gln64) retain a covalently interacting water molecule (Evans et al., 1994). Distal His-E7 of bovine Mb was substituted for Asn and Gln to establish a system where hydrogen bonding interaction between the distal residue and bound-ligand can be altered by changing donor-acceptor distance. The model confirms that hydrogen bonding with the distal residue is a dominant factor for determining the ligand dissociation

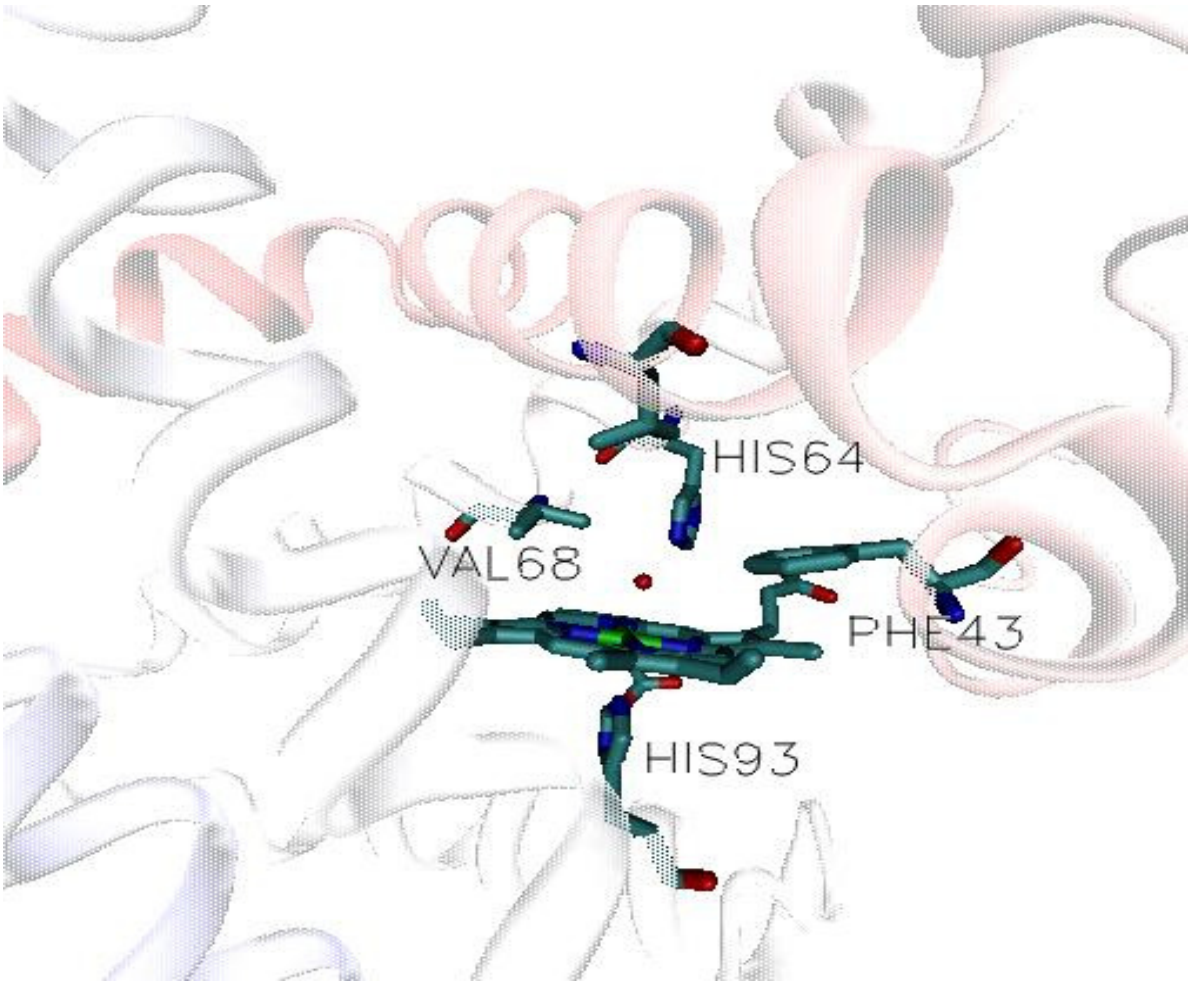

Figure 1.4 Structure of horse heart metmyoglobin from 1YMB pdb **(**Evans et al., 1990).

rate, whereas steric hindrance exerted by the distal residue is a primary determinant for the ligand association (Rajarathnam et al., 1991).

Some notable differences between the active site of a typical peroxidase like HRP and Mb are the absence of an Arg in the pocket in myoglobin that is present in HRP. If we compare the positions of the distal amino acids of both heme enzymes, it is found that they are different, which suggests that this change in spatial position is a specific specialization in each protein for their natural ligands. In the case of Mb, these positions are optimized for transporting oxygen and for HRP to catalyze hydrogen peroxide. Even having some key differences with peroxidases active site, Mb is capable of having some peroxidase activity and reacts with hydrogen peroxide. The active site of myoglobins and hemoglobins share many physical, spectroscopic, and chemical similarities with the active site of peroxidases (Wan et al., 1998).

1.3 Myoglobin acting as peroxidase

The mechanism for the reaction of hydrogen peroxide with peroxidases and myoglobin has historical importance. These reactions are related to oxidative stress and pathophysiological complications in diabetes, atherosclerosis, cancer, and aging in cells (Bursell and King, 2000). Oxidative processes, which are in many cases enhanced when modifications are introduced, lower the oxygen affinity; can limit the safety of hemoglobins for oxygen-carrying therapeutics. The knowledge of the hemoglobins reaction with hydrogen peroxide can help us to overcome the limit impose by these reactions in the development of proteins for oxygen carrying therapeutics. In the reaction of met-myoglobin with H_2O_2, a protein derivative similar to compound I in peroxidases is formed and capable of oxidizing a

wide arrange of substrates (Wan et al., 1998). Ferric myoglobins and hemoglobins undergo a two-electron oxidation in its reaction with H_2O_2. In the mechanism proposed by Poulos and Kraut this reaction occurs in multiple steps. First, the H_2O_2 complexes with the heme then the O-O bond is heterolitically cleavage oxidizing Fe (III) to a protein radical heme Fe^{IV}=O ferryl species known as compound I which rapidly decay in the ferryl species known as compound II. The compound II species is then slowly reduced back to the ferric state by unknown mechanisms. In Figure 1.5 we have the mechanism proposed for the reaction of H_2O_2 with HbI of the clam *Lucina pectinata*. In a similar manner to peroxidases and myoglobin, HbI forms ferryl species upon reaction with H_2O_2. HbI showed the ability to stabilize through its unusual heme pocket configuration (Gln64, Phe43, Phe29, and Phe68), the ferryl (heme Fe^{IV}=O)$^{\cdot+}$ compound I a thousand times more than Mb (De Jesus et al., 2001). These ferryl species previously mentioned in the reaction of HbI of figure 1.5 are as well present in the reaction of myoglobin and peroxidase with H_2O_2. These heme ferryl-oxo derivatives play an important role in the design of the heme proteins substitutes of natural hemoglobin (Alayash et al., 1999; Egawa et al., 2000). The compound I species have been characterized for multiple heme proteins, but its theoretical precursor is still in debate. On previous studies, it was found that compound I was formed within the dead time of stop-flow instruments (Prasad and Mitra, 2004). So this means that it is a precursor that can not be measured in the timescales of rapid mixing techniques. Binding kinetics of many ligands with myoglobins has been determined using stopped flow technique or laser flash photolysis. The laser flash photolysis technique has proven to be very useful for the measurement of rapid bimolecular reactions at convenient ligand concentrations. Unlike conventional

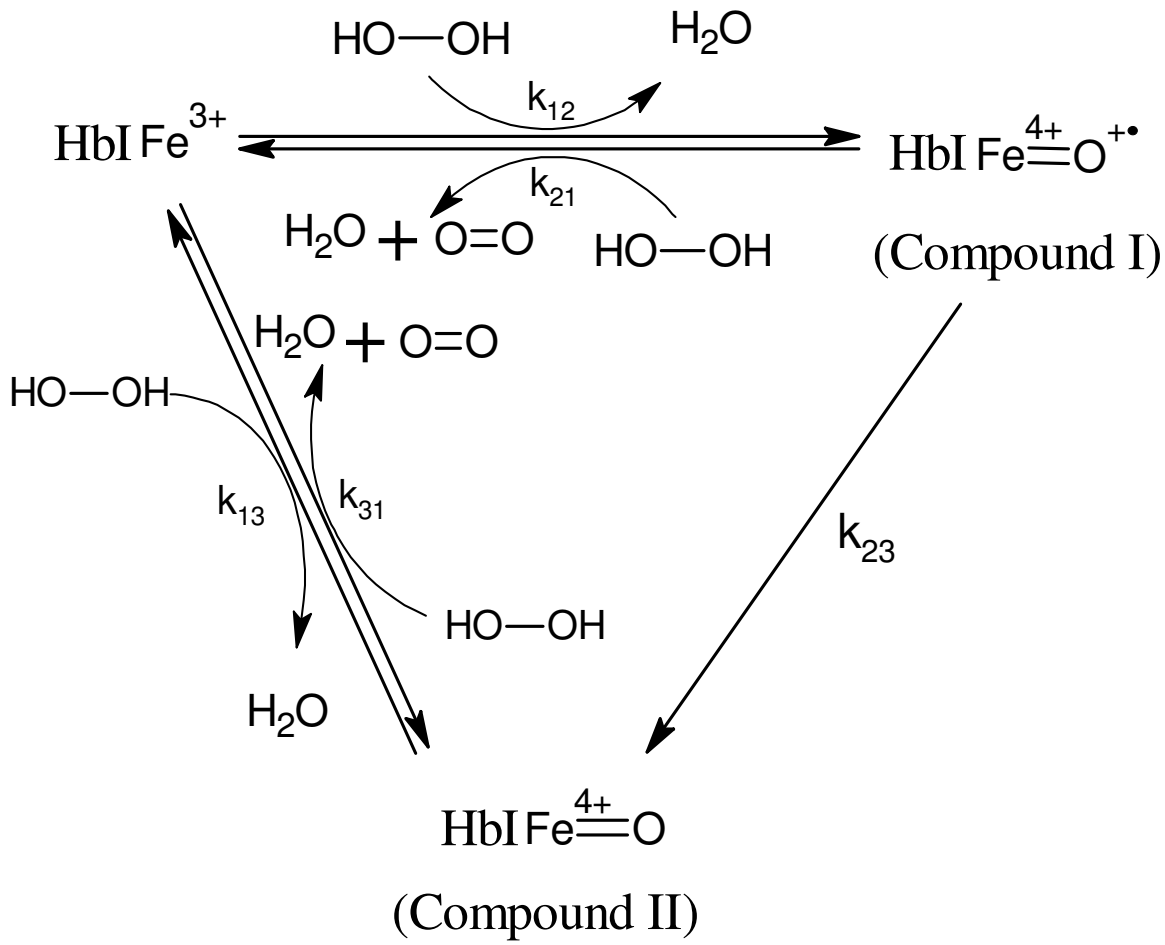

Figure 1.5 Reaction mechanism proposed by for the reaction of *Lucina pectinata* HbI with hydrogen peroxide (De Jesus et al., 2001).

chemical oxidations performed with mixing methods that have a dead mixing time of 1 ms, the photochemical approach produces transient species instantly and direct measurement of this accumulated transients could be relatively straightforward (Zhang et al., 2008). Thus, to determine the transient's events in time scales lower than the rapid mixing techniques for the reaction leading towards of the formation of the Mb ferryl derivatives, it is necessary to develop a photo-induced chemical reaction that can be controlled by a photolytic pulse. In this case, the reaction between MbCO and H_2O_2 should be stable and can be controlled photolytically. Therefore, the formation of ferryl species in Mb now can be followed by monitoring the reaction MbCO and H_2O_2 using pump and probe time-resolved nanoseconds absorption techniques.

1.4 Objective

The main purpose in this project was to detect the compound I species precursor in timescales shorter than millisecond. The results will help to give insight into the questions: What controls Mb reactivity with hydrogen peroxide? Does the heme distal residue control the rate constants for O-O cleavage of the ferryl precursor intermediates? How this correlates or contrasts with other hemoglobins and peroxidases?

2. MATERIALS AND METHODS

2.1 Sample preparation

2.1.1 Met-Myoglobin and myoglobin concentration determination

Myoglobin from horse heart in lyophilized powder (Sigma-Aldrich) sample was diluted in a 200 mM sodium phosphate buffer, and pH of 6.5 and 8.5 was adjusted for each sample. The solution of myoglobin resulted to contain the met-aquo species. To determine the concentration and to verify the identity of the met-myoglobin species, an Agilent 8453 UV-Vis was used. Figure 2.1 shows the characteristic absorption bands for the met-aquo species with a Soret band with maximum at 407 nm, and visible Q bands with maximum at 503 nm and 630 nm and with extinction coefficient of 188 mM^{-1} cm^{-1}, 10.2 mM^{-1} cm^{-1}, and 3.9 mM^{-1} cm^{-1}, respectively (Scheler et al., 1957).

2.1.2 Deoxy-Myoglobin complex and Carbonmonoxy-Myoglobin complex

To prepare the deoxy complex from met aquo-myoglobin (met-Mb), 10 mL of met-Mb with a 195 μM concentration was placed in a sealed vial exposed for about 20 minutes to an anaerobic (N_2) atmosphere with the purpose of removing all the oxygen present in the solution. The solution was kept at approximately 4°C aiming to prevent temperature related sample denaturization. After removal of all the oxygen present in the solution, a 10 mg/ml deoxygenated solution of sodium hydrosulfite (dithionite) was used to reduce the ferric met aquo-Mb species and form the deoxy myoglobin (Mbdeoxy) species. A UV-Vis spectrum was taken with the intention of verifying the deoxy species formation. Figure 2.2 show a

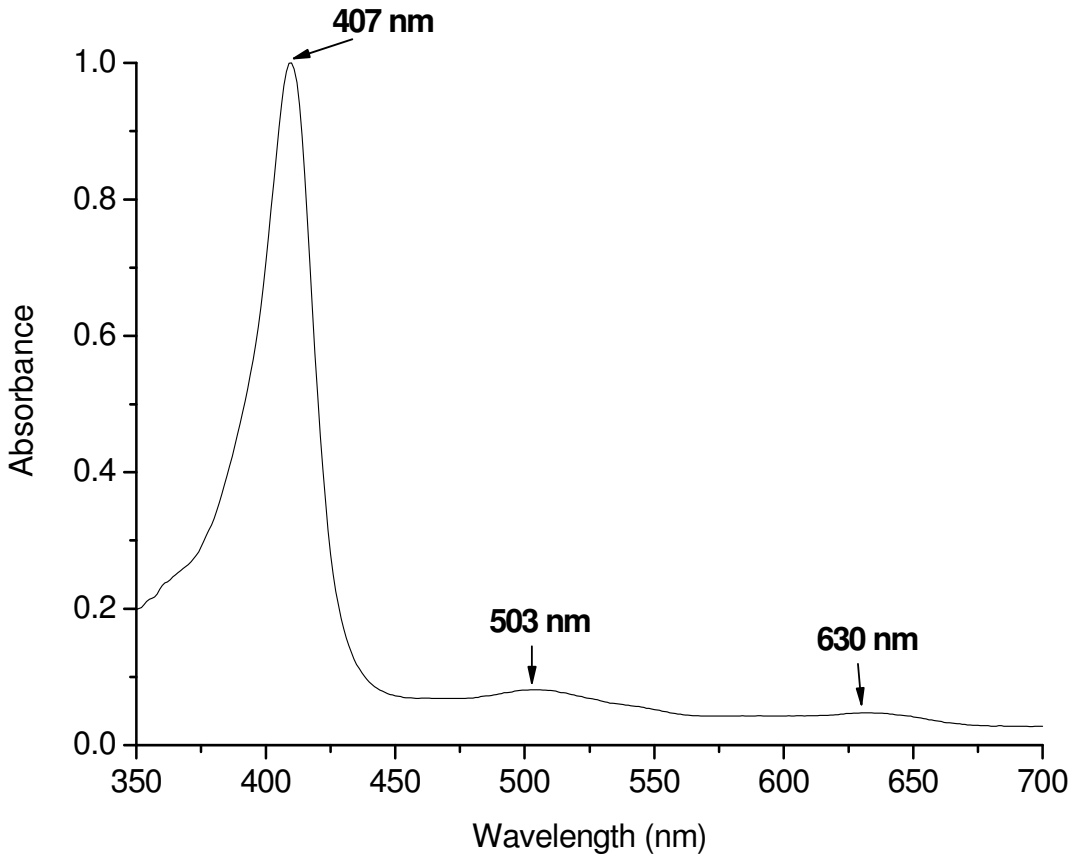

Figure 2.1 UV-Vis spectrum of met-Mb in 200mM sodium phosphate buffer at pH 6.5 with its characteristic Soret band with maximum at 407 nm and Q bands with maximum at 503 nm and 630 nm.

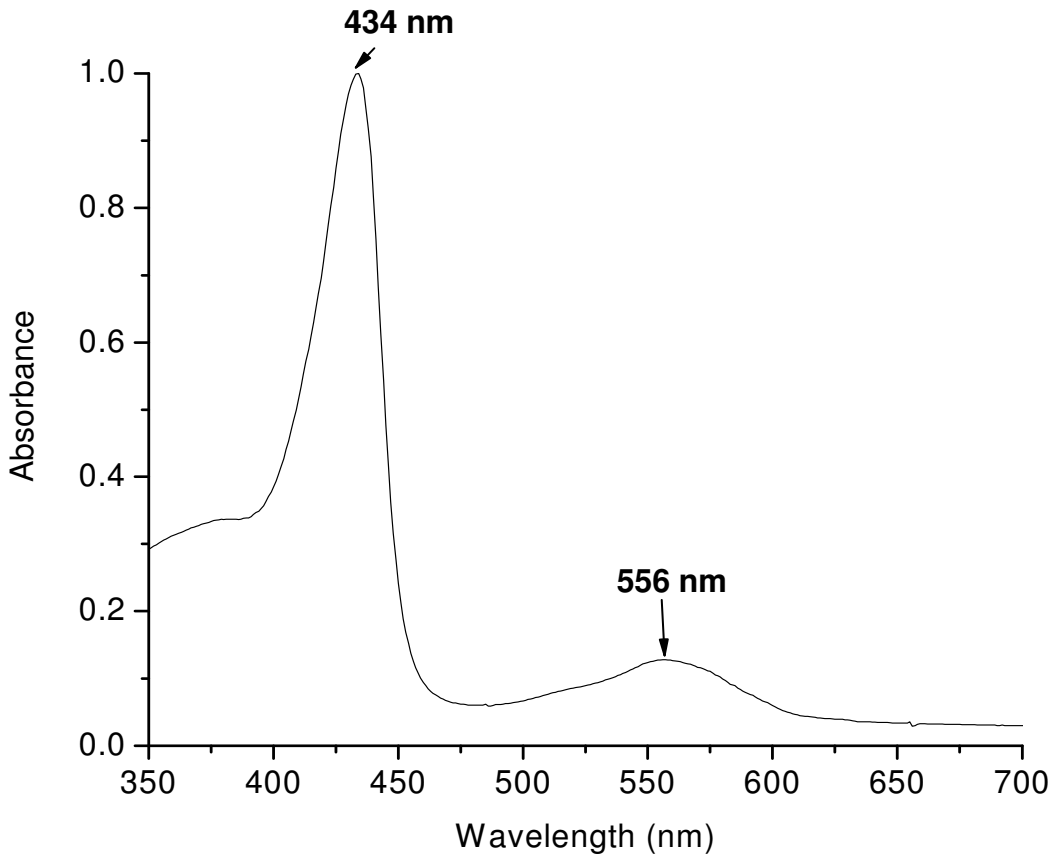

Figure 2.2 UV-Vis spectrum of deoxy-Mb in 200mM sodium phosphate buffer at pH 6.5 with its characteristic Soret band with maximum at 434 nm and Q band with maximum at 556 nm.

distinctive spectrum with Soret band with maximum at 434 nm and a broad visible with maxima at 556 nm (Antonini, 1965). Deoxy Mb samples were equilibrated in a carbonmonoxide (CO) atmosphere for 30 minutes and the carbonmonoxy myoglobin (MbCO) complex was generated. With the purpose of corroborating the formation of MbCO, an UV-Vis spectrum was taken which has Soret band maximum at 422 nm and Q band maximum at 541 and 575 nm (Antonini, 1965). The corresponding spectrum is illustrated in Figure 2.3.

2.2 MbCO complex stability with Hydrogen Peroxide

To study the stability of MbCO complex in solution in the presence of hydrogen peroxide, the behavior of the bands at 422 nm, 541 nm and 575 nm by UV-Vis spectroscopy was monitored. Two samples with pH 6.5 and 8.5 of MbCO were prepared as described before. Each sample consisted of 500 μL of MbCO with a 15 μM concentration placed in a septum sealed cuvette in CO atmosphere witch was later injected with 500 μL of a 15mM concentrated hydrogen peroxide deoxygenated solution to achieve 1:1000 concentration ratio. Exactly after the hydrogen peroxide injection, UV-Vis spectra were recorded for 3 minutes with single UV-Vis spectrum taken every 30 seconds. Figures 2.4 and 2.5 show that there is not a significant change in the MbCO bands intensity, wavelength maximum position nor shape.

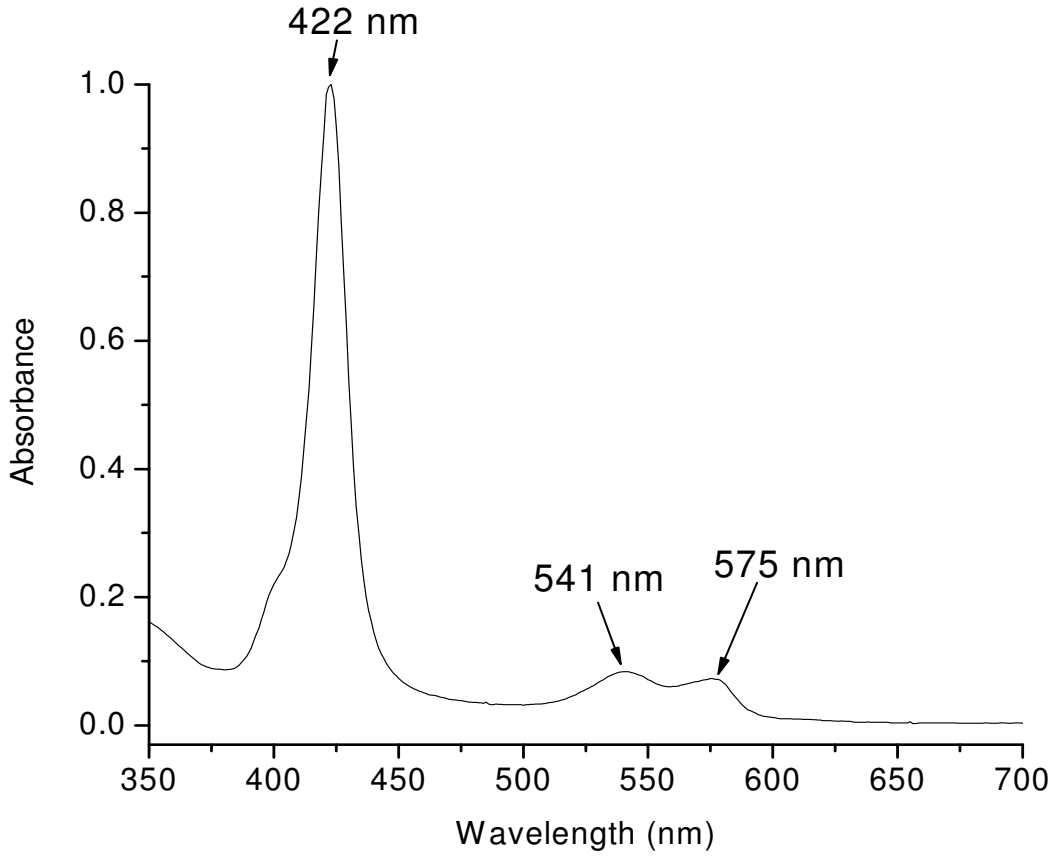

Figure 2.3 UV-Vis spectrum of MbCO in 200mM sodium phosphate buffer at pH 6.5 with its characteristic Soret band with maximum at 422 nm and Q bands with maximum at 541 and 575 nm.

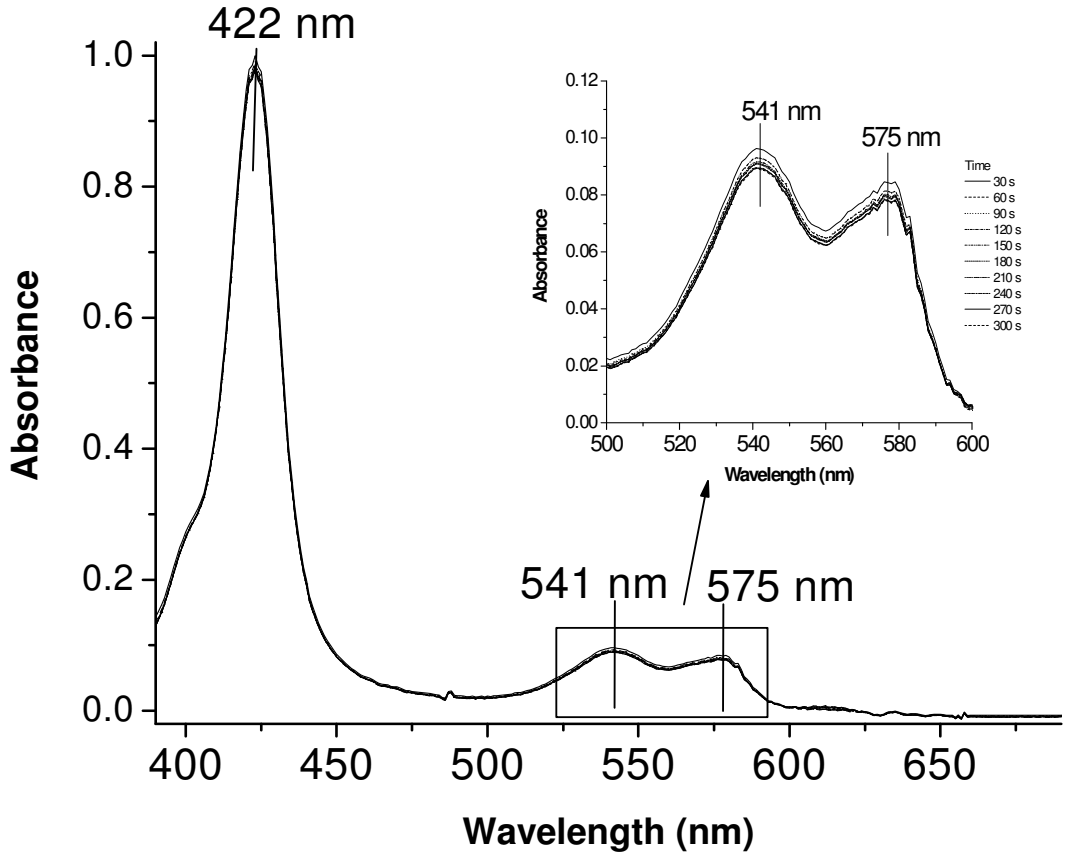

Figure 2.4 Steady state UV-Vis spectra of MbCO with hydrogen peroxide (1:1000 ratio) in 200mM sodium phosphate buffer at pH 6.5. Both spectra set shown are from 30 to 300 seconds.

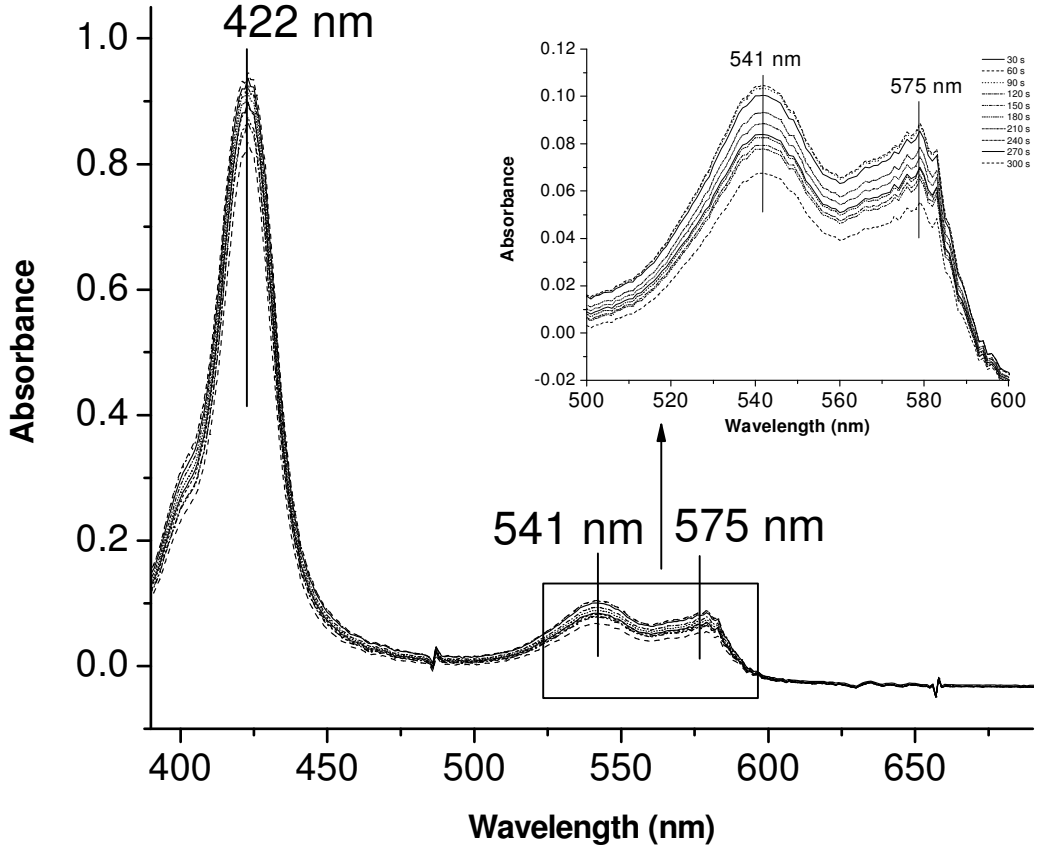

Figure 2.5 Steady state UV-Vis spectra of MbCO with hydrogen peroxide (1:1000 ratio) in 200mM sodium phosphate buffer at pH 8.5. Both spectra set shown are from 30 to 300 seconds.

2.3 Laser flash photolysis

2.3.1 Instrument Set up

A LP920 laser flash photolysis spectrometer from Edinburgh Instruments was used. Figure 2.6, 2.7 and 2.8 show a detailed drawing of the LP920 spectrometer with its parts. The LP920 consist of multiple parts. First, as a probe source, the LP920 has an ozone-free Xe arc lamp of 450 W from Osram ®. The lamp has a continuous spectral distribution ranging from 190 to 2600 nm and is used in pulsed mode. In the sample compartment there are two irises, one to control the amount of light from the probe light to the sample and one to control the amount of light entering to the monochromator slit. Following the iris, there are two focus lenses, one to help focus the probe beam in the sample chamber and the other one to focus the light coming from the sample through the monochromator entrance slit and to the entrance mirror of the monochromator. Also inside of the sample compartment are the probe lamp shutter and the laser shutter. Finally, there is the quasi co-linear sample holder and the mirrors required to redirect the laser beam from the sample holder mirror back to the sample holder at the angle and height desired to intersect the probe light beam at the sample cell chamber. This beam set up is advantageous because of an increase in cross section within the sample. The cross section volume where the probe and laser beam are collimated is of 90 μL and the volume inside the sample cell chamber was of 100 μL. As sample cell, a Hi-tech SFA-20 mixer was coupled to the LP920 spectrometer. The mixer consists of three reactant syringes and one waste syringe. The reagents flow through a thermostated umbilical cord to the cell where they are mixed. The observation cell is made of Spectrasil B fused silica with wavelength observation range of 200 nm to 850 nm and has two optical path length, 2 mm

and 10 mm, but the 2mm was preferred in order to be able to use lower concentration. Connected to the sample compartment is the monochromator, a symmetrical Czerny-Turner monochromator. It has two (2) plane reflection gratings. One of the gratings has 1800 grooves/mm, it is usually used for the kinetics analysis using a PMT as detector and it has wavelength coverage range of 200 nm to 900 nm. The second grating has 300 grooves/mm and is used in conjunction with a CCD camera offering a wavelength coverage range of 250 nm to 900 nm. As detection system, an Andor Technologies *i*-Star DH720 CCD camera with a spectral range of 180 nm to 850 nm, was used. The system has, as a pump source, a 25 mJ pulse with a 532 nm wavelength and 7 ns pulse width from a Surelite II Nd:YAG laser from Continuum®.

2.3.2 Time set up

Integration of the different parts in time is critical for all the pump and probe experiments. In this system, all components are time integrated by the LP920 controller, and time adjustment for all parts can be adjusted from the system's PC. Figure 2.9 shows an example of the time sequence integration inside the LP920 and the integration of it with the SFA-20. In the next sentences, the time sequence will be described in detailed as is showed in Figure 2.9. The flash delay purpose is to adjust the laser flash lamp firing at the flattest part of the lamp profile to acquire the measurement. This ensures that changes in sample absorption are because of transient's population change and not changes due to in intensity of the lamp. The flash lamp delay in the experiment was set up to 5 ms, this locates the laser firing in the middle of the 10 ms probe lamp profile which is the flattest part of the lamp profile for this instrument set up. The q-switch trigger delay for the Surelite II used is

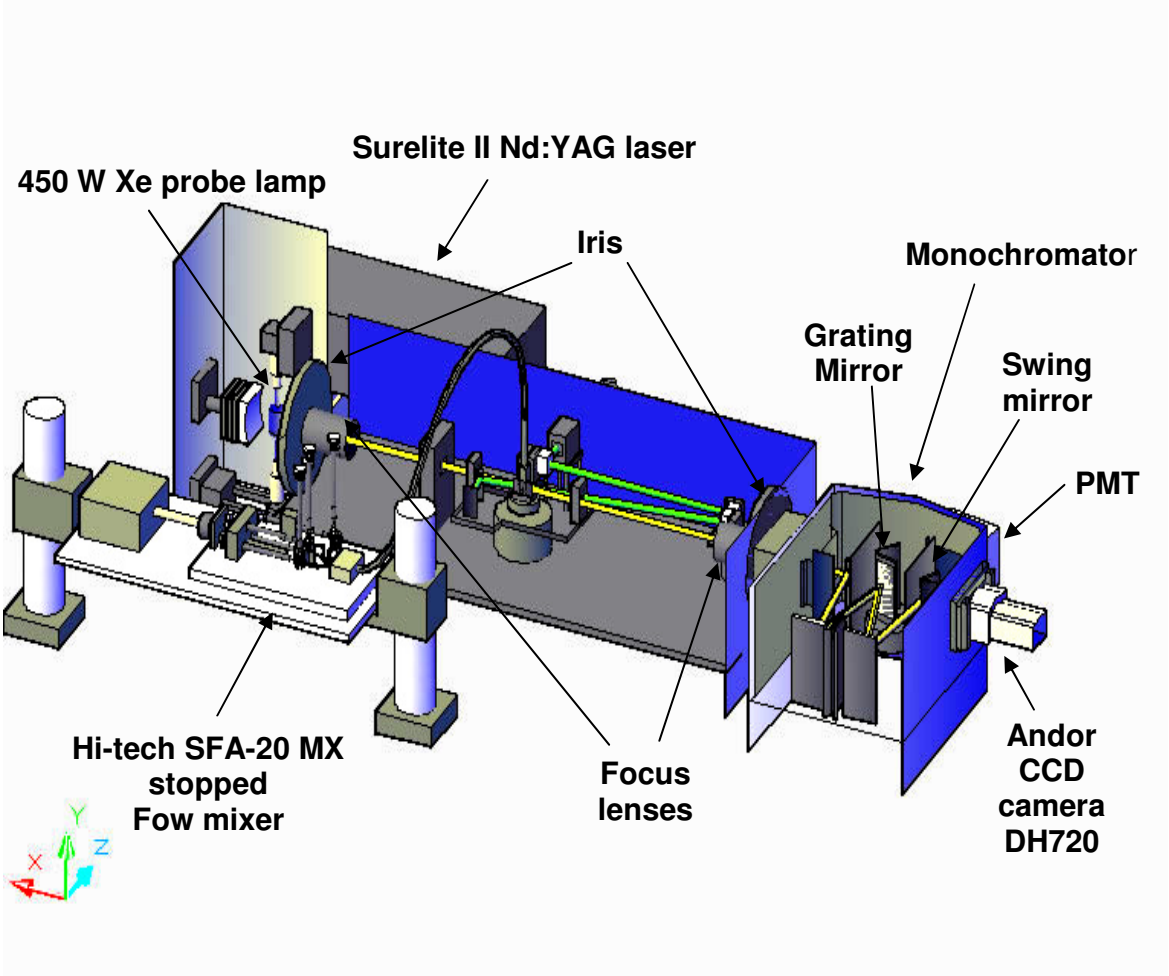

Figure 2.6 LP920 instrumental setup.

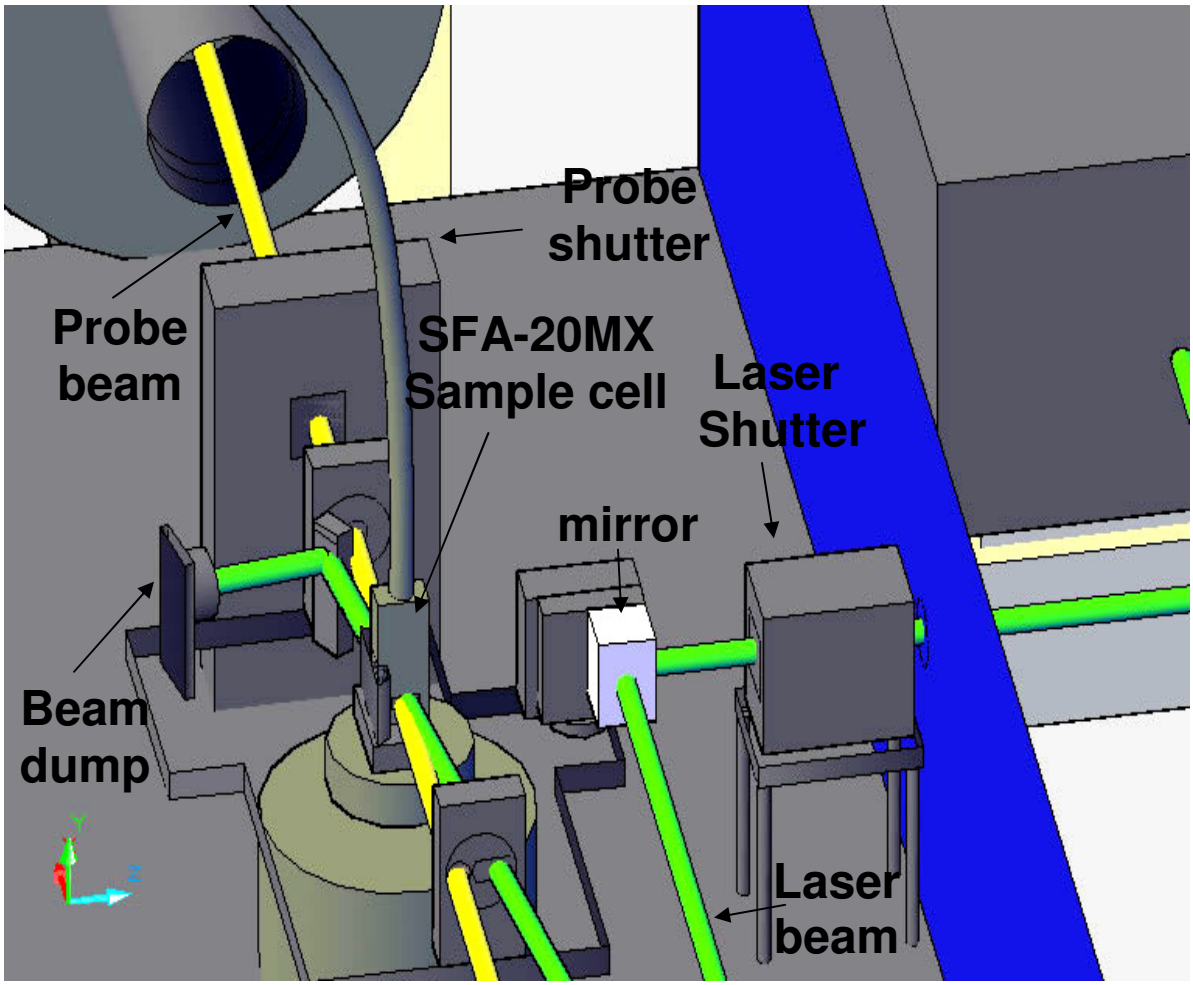

Figure 2.7 LP920 sample chamber with SFA sample cell in place with probe and laser beam crossing at sample cell window.

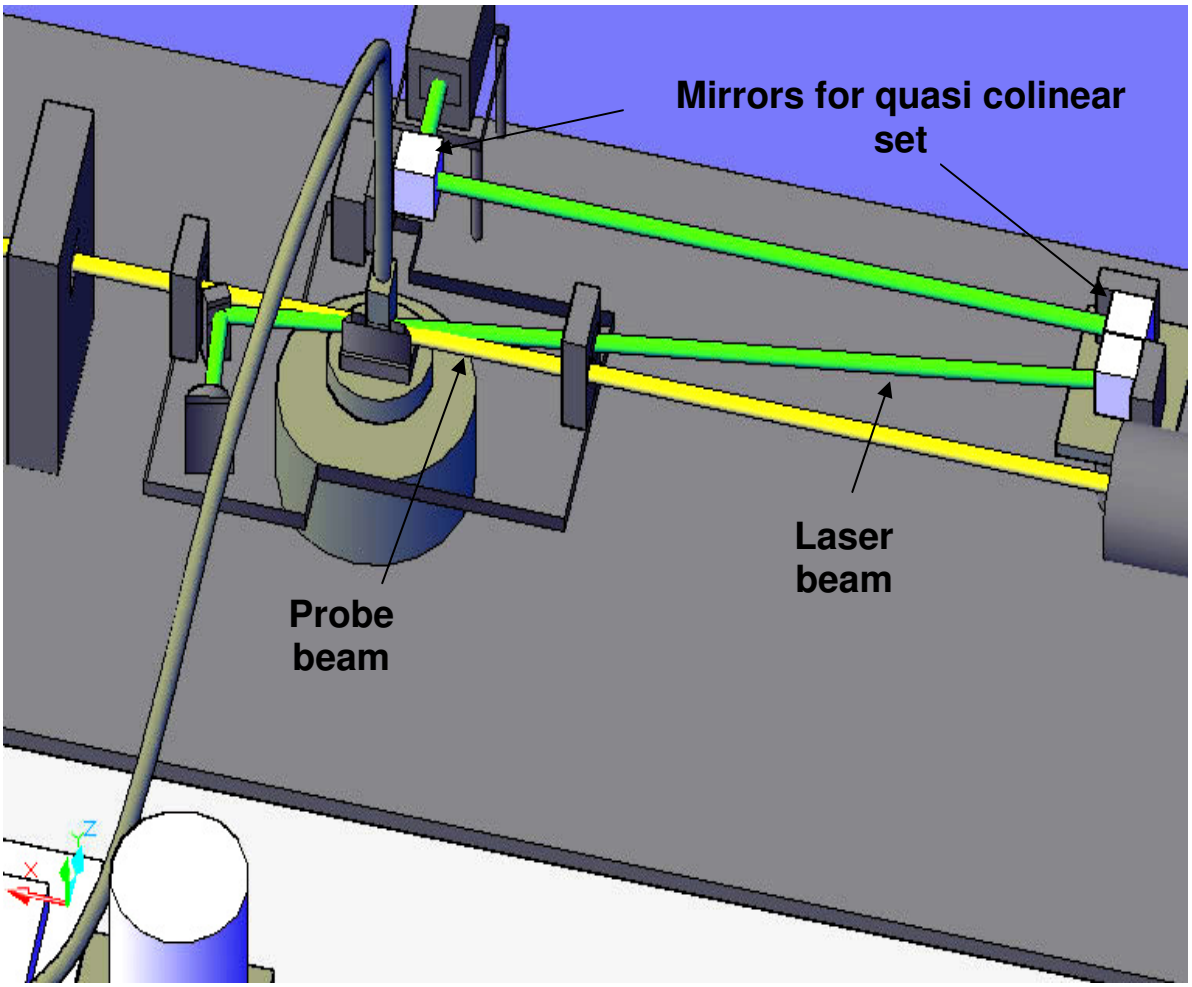

Figure 2.8 Top view of the LP920 sample chamber with SFA sample cell in place with probe and laser beam crossing at sample cell window and showing all quasi collinear mirrors.

200 μs. Next is the SFA-20 stopped flow trigger. The SFA-20 mixer is connected to the LP920 controller through a delay generator which permits adjusting the time one mixes the reactants prior to the flash event. As presented in Figure 2.9, the first delay was of 50 ns plus 500 μs plus the mixer dead of 10 ms. This allows the reactants be mixed 1.65 ms prior to the laser flash firing. The laser shutter and probe shutter are open for around 12 ms to give enough time for the probe and laser light to completely pass through. For the detection integration using the *i*CCD camera, a *iCCD* delay was incorporated to compensate for the camera 7ns rise time and the final delay for the experiment. This final delay is first adjusted to be at very end of the laser pulse. If a single line at 532 nm is observed in the set up spectra, one needs to increase the delay until the flash line disappears. With this *i*CCD final delay adjusted, one can proceed to change to the acquisition mode in which one establishes the desired time window and steps increments for the experimental window. The instrument maximum time resolution was of 10 ns and the maximum time window width is from 0 to 5 ms. In the experiment the time steps are of 60 ns and the time window is varied from 0-600 ns. For each single time step spectrum, fresh sample was injected by the SFA-20 stopped flow mixer. The time resolved spectrum is an average of three (3) spectra. This is repeated through the entire time window previously mentioned. All time resolved spectra have signal resolution of 0.002 ΔOD and were recorded at 25°C. In order to verify at which wavelength was located a shoulder or peak, a second derivative was taken to all spectra.

2.3.3 MbCO laser flash photolysis recombination

After the laser pulse breaks the bond between CO and heme iron in Mb the protein

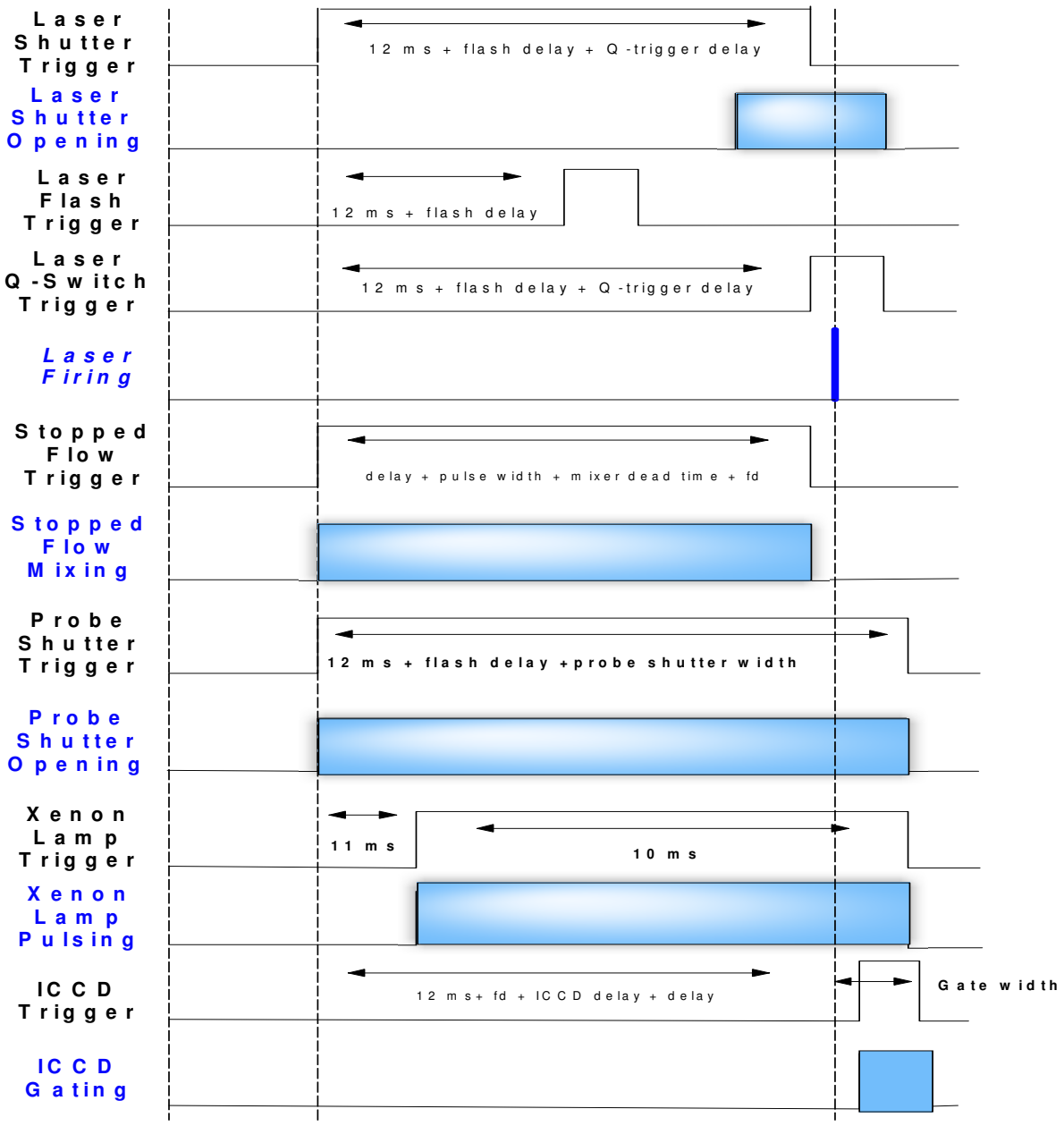

Figure 2.9 Time events schedule for equipment integration.

goes to a metastable intermediate (Mb*), and CO moves away from the heme (Levantino et al., 2004). The CO rebinding with heme is then monitored by UV-Vis through time. Figure 2.10 shows the time resolved absorption difference spectra between Mbdeoxy and MbCO. The 435nm and 559nm peaks correspond to the Soret and Q-band for the deoxy Mb species, respectively. As the amount of Mbdeoxy species decreases through time and the CO rebinding increases with Mb heme, the 435 nm (Soret) and 559nm (Q-band) peaks decreases in intesity in the direction stated by the arrows in Figure 2.10. The 420nm, 538nm and 579nm negative peaks in Figure 2.10 stand for the Soret (420nm) and Q-bands (538nm, 579nm) of MbCO. As the amount of deoxy species decreases through time the 435 nm positive peak in Figure 2.10 goes from positive to zero in the direction which is shown by the arrow. In the case of the MbCO peak at 420nm, it goes up from negative to zero, as illustrated by an arrow in Figure 2.10. Spectra in Figure 2.10, each represent a snapshot in time, taken every 100 μs after photolysis. If one takes the static UV-Vis spectrum of Mbdeoxy and subtract the MbCO spectrum one finishes with a difference spectrum similar to the time resolved difference spectrum taken for one time step snap shot. This can be appreciated in Figure 2.11 which the difference is obtained when MbCO spectrum is substracted from the Mbdeoxy spectrum.

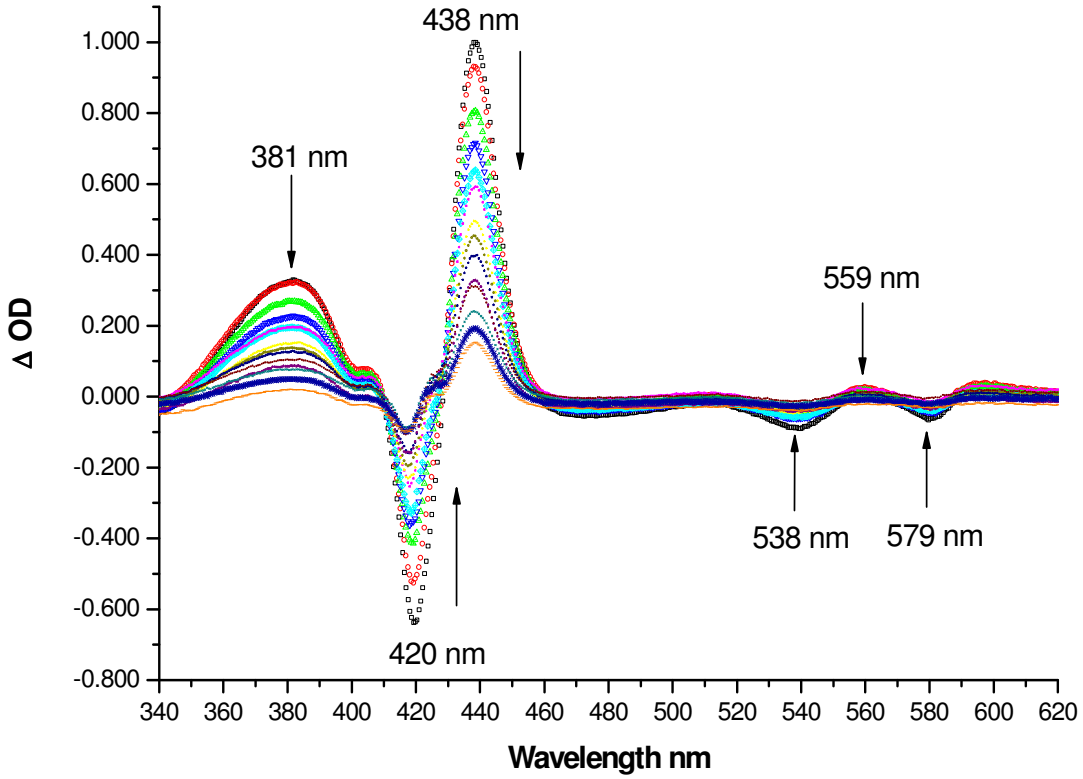

Figure 2.10 Laser flash photolysis UV-Vis difference spectra of MbCO in 200mM sodium phosphate buffer at pH 6.5. The 435nm and 559nm peaks correspond to the Soret and Q-band for Mbdeoxy species, respectively. The 420nm, 538nm and 579nm negative peaks stand for the Soret (420nm) and Q-bands (538nm, 579nm) of MbCO. The peaks decrease with time in the direction of the arrows. The spectra time window goes from 0(black) to 1400 μs (orange) after photolysis. The spectra resolution was of 0.002 ΔOD

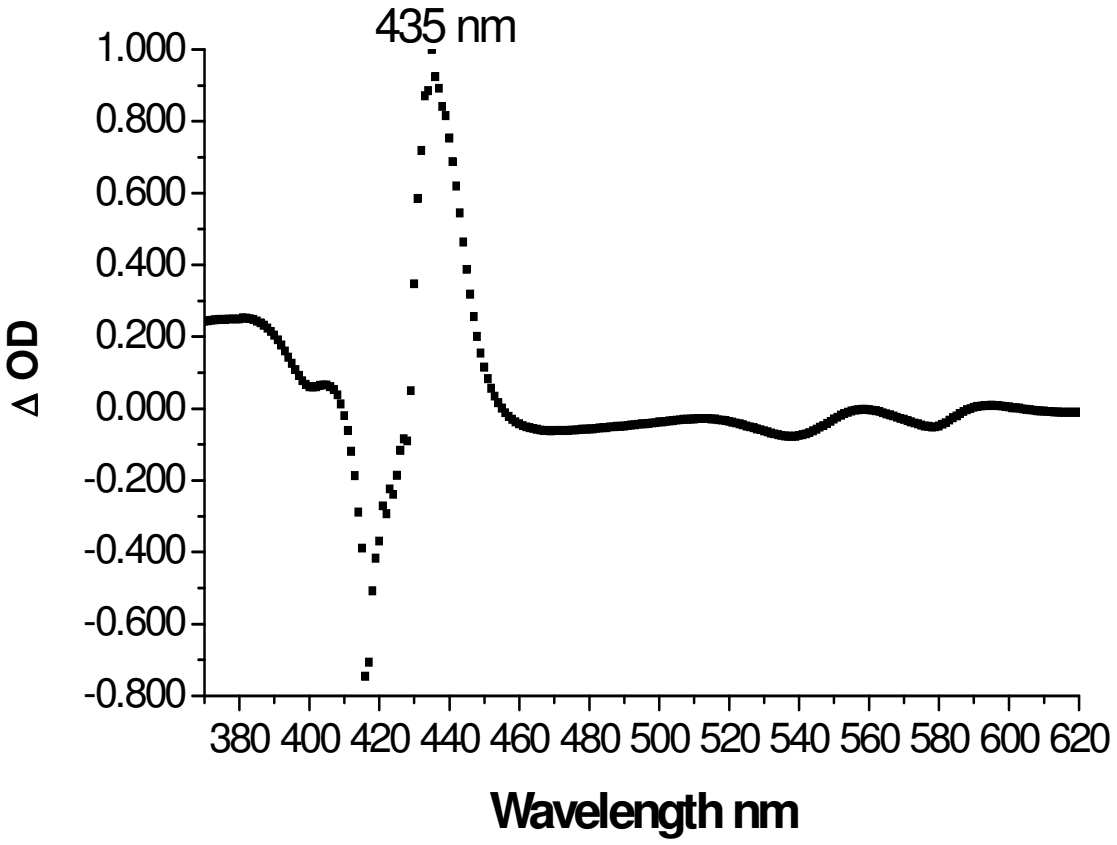

Figure 2.11 Mbdeoxy-MbCO UV-Vis steady state substraction spectrum in 200mM sodium phosphate buffer at pH 6.5.

3. RESULTS AND DISCUSSION

3.1 Recombination of MbCO after laser flash photolysis in nanoseconds

The time resolved UV-Vis spectrum of MbCO in the nanoseconds timescale at 25°C is presented in Figure 3.1. The timescale for the spectrum is between 50 to 600 ns in steps of 50 ns each, that shows the 438 nm band corresponding to the deoxyMb and the 423 nm shoulder identified as the geminate MbCO complex. In the insert shown, the ΔOD of the 423 nm shoulder shows no significant change during the spectrum timescale. This small shoulder at 423 nm has been attributed to a geminate recombination of CO with Mb. The geminate recombination is observed in flash photolysis experiments of many hemeproteins including Mb. In this process, the CO or any other photodissociated ligand in the heme poceket or the protein matrix rebinds to the heme without escaping to the solvent region (Sugimoto et al., 1998). This behavior is accredited to packing imperfections of the protein matrix which creates mainly hydrophobic cavities known as Xenon pockets. These pockets volume range between 30-100 $Å^3$. Their positions are near the heme active site. The Xe_1 is located at the proximal site, while Xe_4 is at the distal site, Xe_3 is near the protein surface, and Xe_2 is in an intermediary position between Xe_4 and Xe_1. Ultrafast dynamics experiments with the hemoglobins I and II from clam *Lucina pectinata* having CO as a ligand shows that distal amino acids configuration affects geminate recombination process. For example HbICO has a recombination time of around 9.2 ps compare to HbII 3.0 ps (Rodriguez, M., 2005). Similar to this behavior (Sugimoto et al., 1998) it's been found that changing the

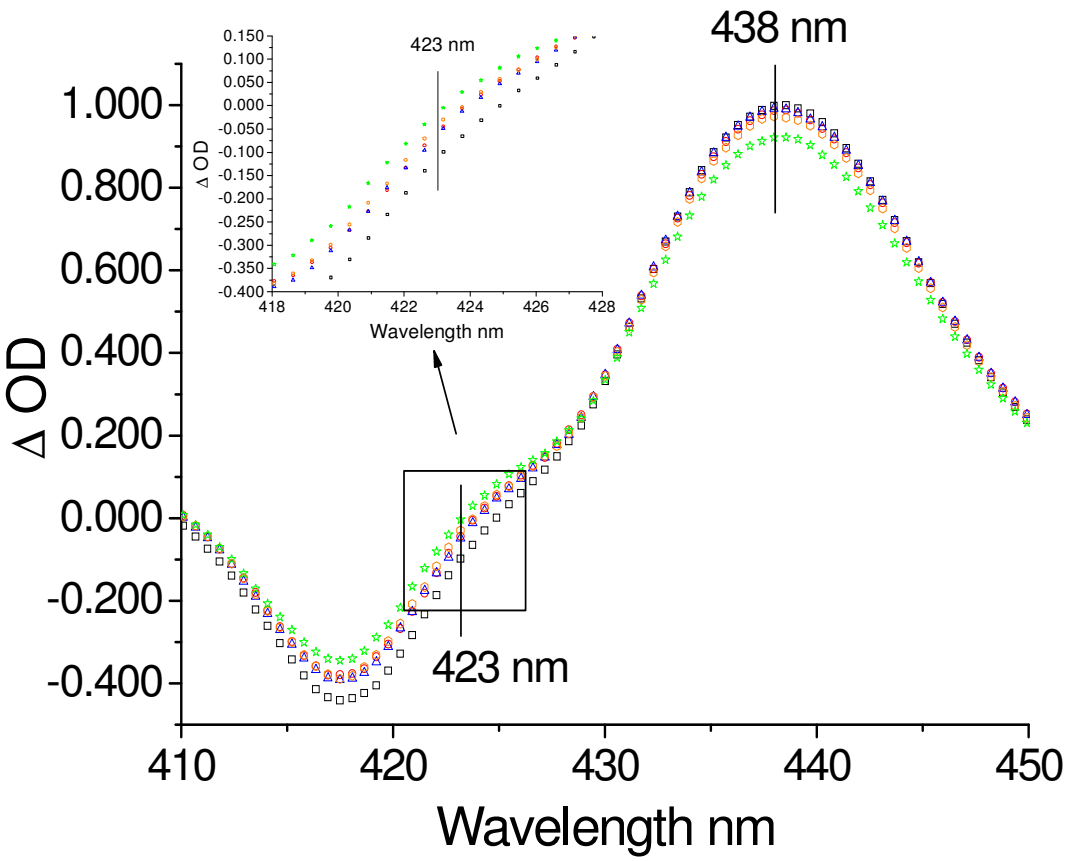

Figure 3.1 MbCO UV-Vis time resolved difference spectrum in 200mM sodium phosphate buffer at pH 6.5. The spectra time steps are: 50 ns (black squares), 150 ns (red circles), 300 ns (blue triangle) and 450ns (orange hexagons) and 550 ns (green stars). The spectra resolution was of 0.002 ΔOD.

distal amino acids makes a significant change in the proportion of geminate recombination percent versus the bimolecular recombination percent. Their results show that an effect in the mutation from polar groups to non polar groups like in the H64V mutation increases significantly the geminate recombination yield. Their reported values for wild type Mb are around 7% for the nanosecond recombination, and the bimolecular recombination accounts for the remainder 93%. When this wild type Mb numbers are compared to the H64V/V68T double mutant, this have present around 10 fold more geminate recombination. This evidence supports the idea that the small shoulder present at 423 nm is a small percentage of nanosecond geminate recombination. Because most of the photolysed CO escapes to the solvent and the CO does interfere in our experiment time window because it returns later in the microsecond timescale. This could be the reason why the spectrum does not reflect a change in shoulder intensity neither shoulder shape in the spectra in Figure 3.1.

3.2 MbCO with H_2O_2 laser flash photolysis in nanoseconds

Figure 3.2 shows 195 μM MbCO with 1.95 mM hydrogen peroxide UV-Vis time resolved difference spectrum in 200mM sodium phosphate buffer at pH 6.5. The spectra time steps are: 60 ns, 120 ns, 300 ns, 420ns and 540 ns. In the insert, can be seen the 424 nm band is indeed blue shifting towards 422 nm during the spectrum timescale. The photolysis of MbCO in the presence of H_2O_2 in Figure 3.2 is compared to the MbCO photolysis spectrum in Figure 3.1 and it has several key differences. First, there is a peak at 424 nm instead of a small shoulder at 423 nm and second the 424 nm bands blue shifts in the time window of the spectrum to 422 nm. This difference suggests that the changes between both spectra are because the presence of a transient species upon reaction of Mb with H_2O_2.

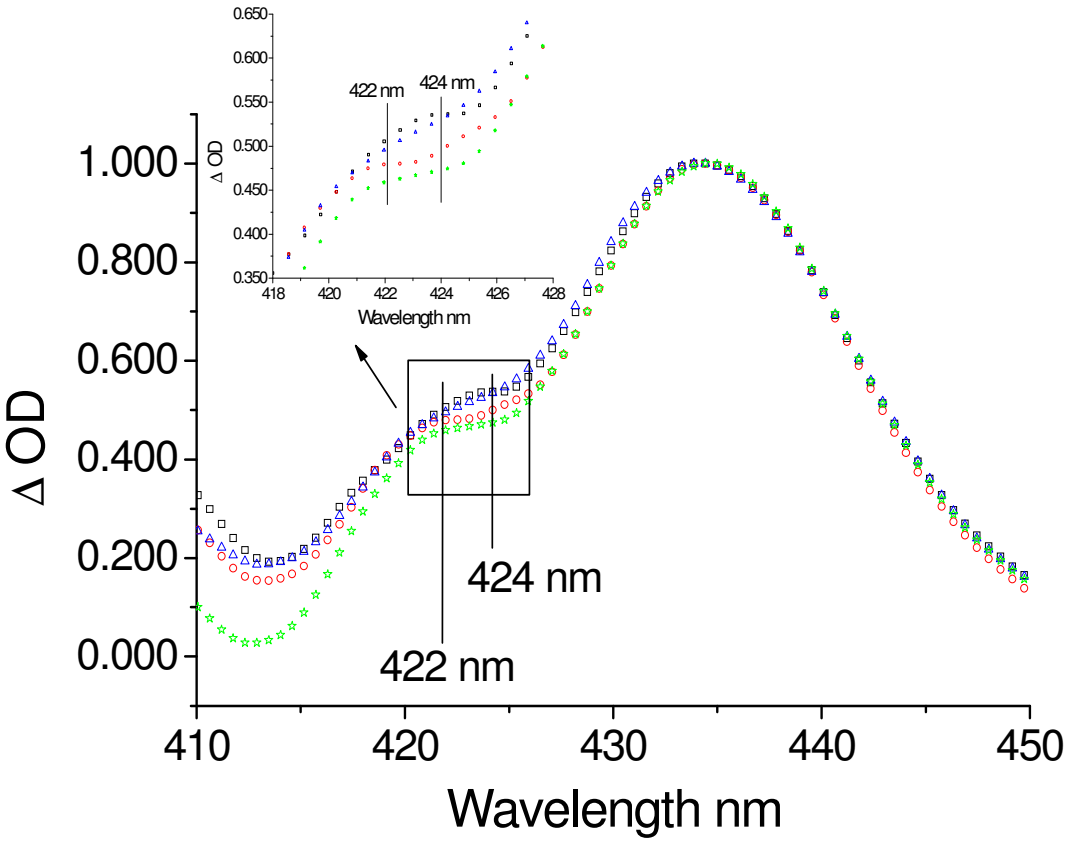

Figure 3.2 UV-Vis time resolved difference spectrum of 195 μM MbCO with 1.95 mM hydrogen peroxide in 200mM sodium phosphate buffer at pH 6.5. The spectra time steps are: 60 ns (black squares), 120 ns (red circles), 300 ns (blue triangle) and 420ns (orange hexagons) and 540 ns (green stars). The spectra resolution was of 0.002 ΔOD.

Since this is a second order reaction, the hydrogen peroxide concentration can be increased at a constant concentration of the MbCO, allowing us examine the behavior of this reaction. Figure 3.3 shows the spectrum of MbCO with H_2O_2 in a 1:500 concentration ratio. This spectrum has a more pronounced 424 nm peak which blue shifts to a final wavelength of 422nm in the same time window. Similarly, Figure 3.4 presents the spectrum for the reaction of MbCO with H_2O_2 in a 1:1000 concentration ratio. The data presents a small peak at 422 nm, but it does not have any significant similarity with the observed in Figure 3.1. These changes in spectra bands with increased hydrogen peroxide concentration provide evidence about the formation of an intermediate upon the reaction between hydrogen peroxide and the photolysis product of deoxyMb.

To define which of the reaction transient(s) can explain the data it is necessary to look at the reaction sequence in Figure 1.5 (on page 15). First the reaction of metMb with H_2O_2 generates the Compound I (heme FeIV=$O^{\cdot+}$) species. This ferryl π-cation radical derivative or Compound I decays through the acceptance of an electron from the protein to form the heme ferryl Compound II (heme FeIV=O) derivative. However, the reaction between deoxy Mb and H_2O_2 always lead directly to the formation of the ferryl Compound II. This is because the extra electron on the deoxy heme species precludes the formation of the (heme FeIV=$O^{\cdot+}$) species or Compound I. Previous studies have established that the Compound II species for Mb has a Soret around 421 nm with visible bands around 551 nm and 586 nm and Compound I has a characteristic broad Soret band around 418 nm with visible prominents peaks around 550 nm, 590 nm and 648nm (Egawa et al., 2000). This 648 nm visible band is

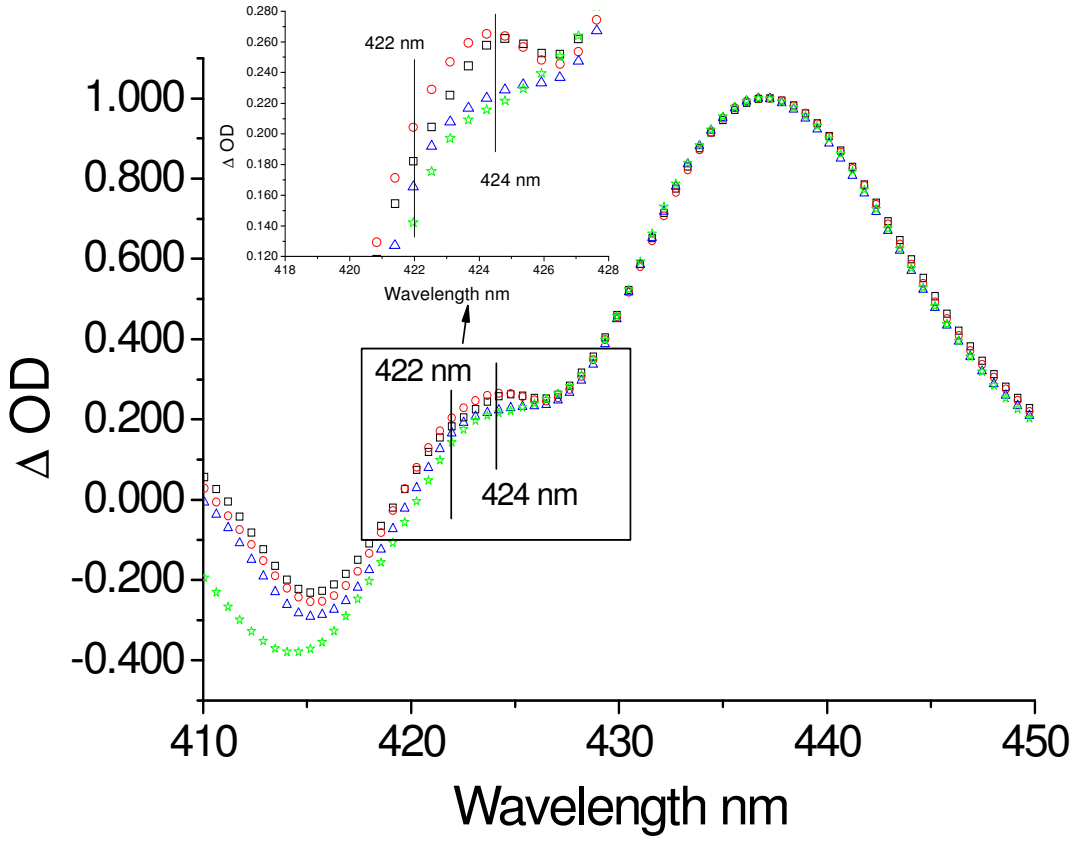

Figure 3.3 UV-Vis time resolved difference spectrum of 195 µM MbCO with 97.5 mM hydrogen peroxide in 200mM sodium phosphate buffer at pH 6.5. The spectra time steps are: 60 ns (black squares), 180 ns (red circles), 300 ns (blue triangle) and 540 ns (green stars). The spectra resolution was of 0.002 ΔOD.

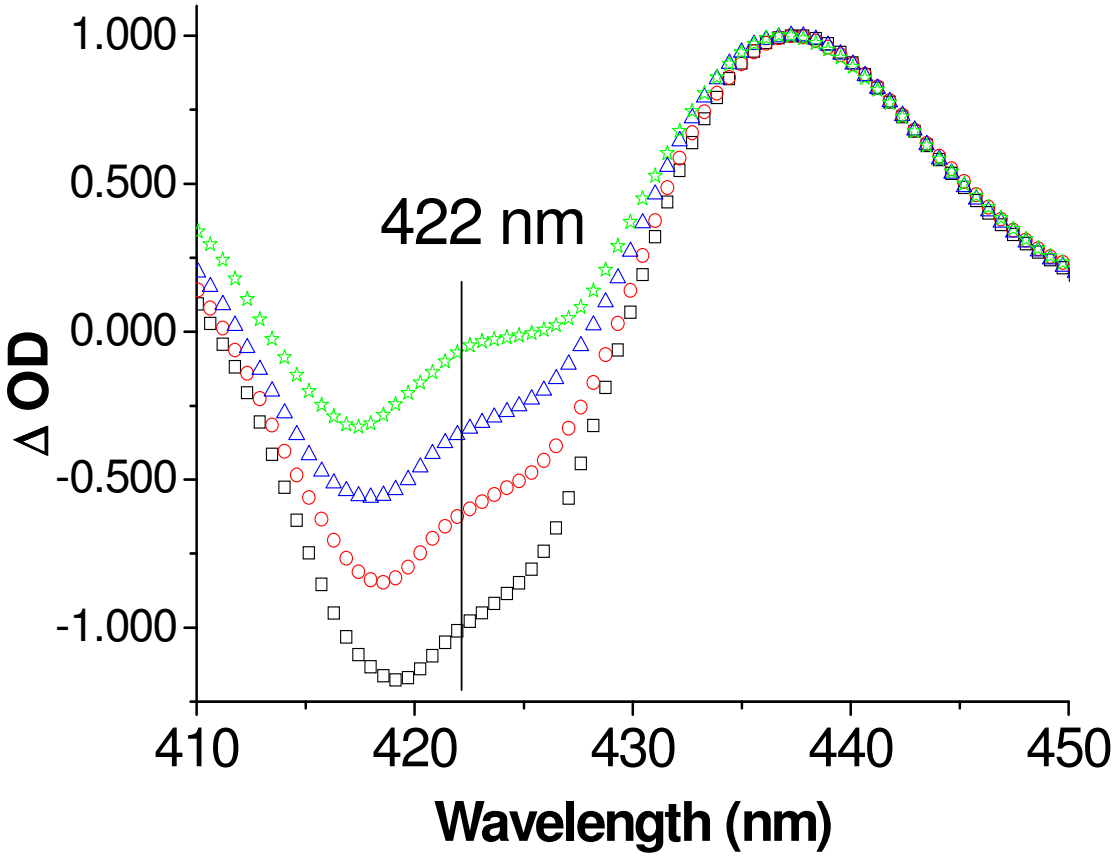

Figure 3.4 UV-Vis time resolved difference spectrum of 195 μM MbCO with 195 mM hydrogen peroxide in 200mM sodium phosphate buffer at pH 6.5. The spectra time steps are: 60 ns (black squares), 180 ns (red circles), 300 ns (blue triangle) and 540 ns (green stars). The spectra resolution was of 0.002 ΔOD.

very characteristic of compound I and it is present in other hemeproteins. In our transient's studies, this 648 nm visible band was not observed, supporting the hypothesis that the reaction between deoxy Mb and H_2O_2 always leads directly to the formation of the ferryl Compound II. This data helps to eliminate the Compound I species as the possible transient presents in the 424 nm band.

However, Compound II species could explain the 422 nm Soret band in the Figure 3.4 and spectra the shoulders in Figures 3.2 and 3.3. On the other hand, because the lifetime Compound II species is much longer than the observed transient intermediate, it can be suggested that a precursor named compound O (heme Fe^{3+}-OOH^-) or ferric heme-hydroperoxide (heme Fe^{3+}-H_2O_2) maybe responsible for the observed 424 nm derivative. This Compound O have been previously proposed as a precursor for the Compound I species (Poulos and Kraut, 1980), being the formation for the Compound I the rate limiting step in the peroxidative reaction (Wan et al., 1998). The formation of the Compound 0 is also suggested to be the initial step in the reaction of hydrogen peroxide with cytochrome P450 and other heme proteins (Matsumura et al., 2008). The Compound O species is really a resonance system between the following species including the heme hydroperoxide species.

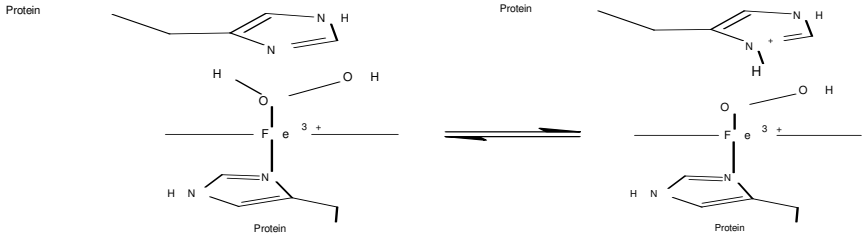

f e r r i c h e m e
h y d r o p e r o x i d e
4 2 6 n m

C o m p o u n d 0
4 2 6 n m

Furthermore, Figures 3.5, 3.6 and 3.7 show the difference spectra between the data in Figure 3.1 and Figures 3.2, 3.3, and 3.4 respectively. The differences between the spectra allow, in part, to eliminate the contribution of the MbCO geminate recombination to each transient spectrum. Thus, Figure 3.5 and 3.6 presents a peak at 426 nm attributed to Compound O. As the concentration is increases as presented in Figure 3.7 there is the presence of a new band which can be attribute to the Compound II derivatives.

Furthermore, Egawa and collaborators (Egawa et al., 2003) applying singular value decomposition to stop flow data from the reaction between metMb and hydrogen peroxide found in their spectra that one of the components suggested to give rise to the detected peak was Compound II and the other accredited to an unknown species is suggested to be Compound 0. Also through EPR spectroscopy experiments, for the hydroperoxy compound they report g values of 2.32, 2.19 and 1.94. These values serve as an unmistakable signature of the Compound 0 structure. This data estimate that the accumulated amount of Compound 0 intermediate was 2 orders of magnitude smaller relative to the Compound II species. The existence of the Compound 0 species has not been directly identified by freeze quench methods neither ultrafast micromixing devices with resolution of microseconds. This is because the Compound 0 species lifetimes has been suggested to be shorter than microseconds. Possibly attributed that the distal histidine in the position E7 of the heme proteins becomes an unstable imidazolium cation after accepting a proton from the H_2O_2 (Shintaku et al., 2005; Tanaka et al., 2004).

Therefore, until our work no previous research has been able to identify or produce evidence about the presence at room temperature (25°C) of the Compound 0 complex. These

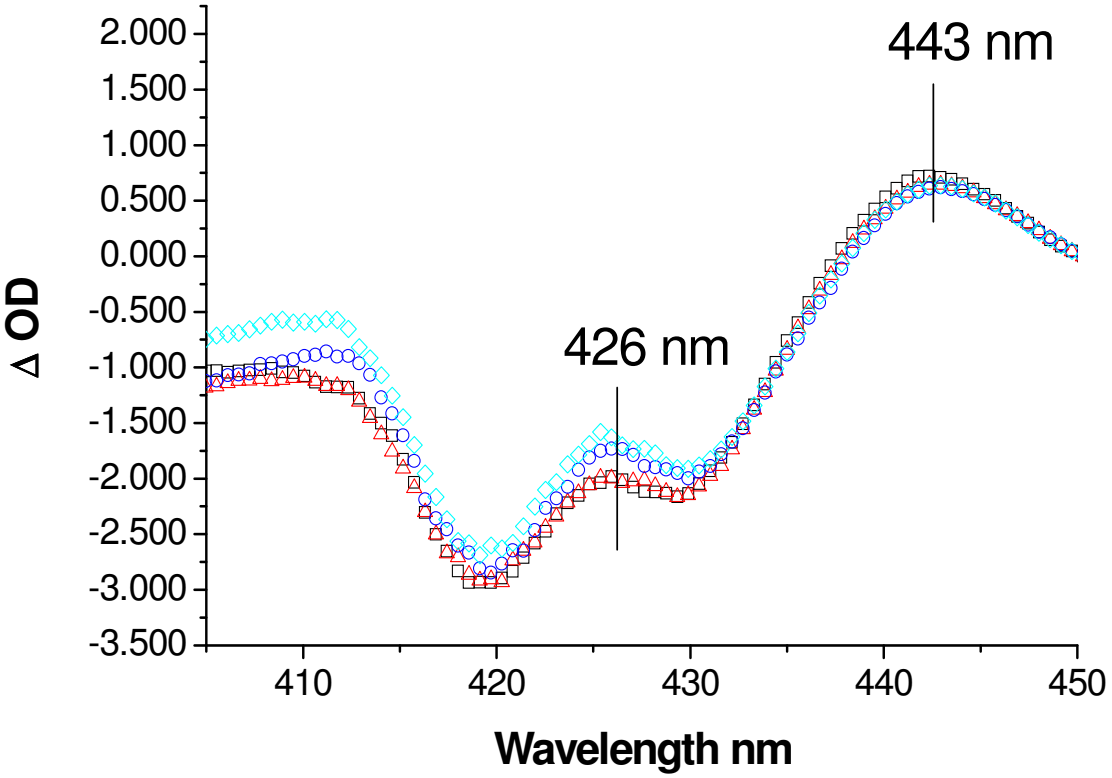

Figure 3.5 Soret band region of 1:10 MbCO and H_2O_2 with CO substracted. Black squares are 120 ns, red triangles 300 ns, blue circles 420 ns and cyan diamonds 540 ns. The spectra resolution was of 0.002 ΔOD.

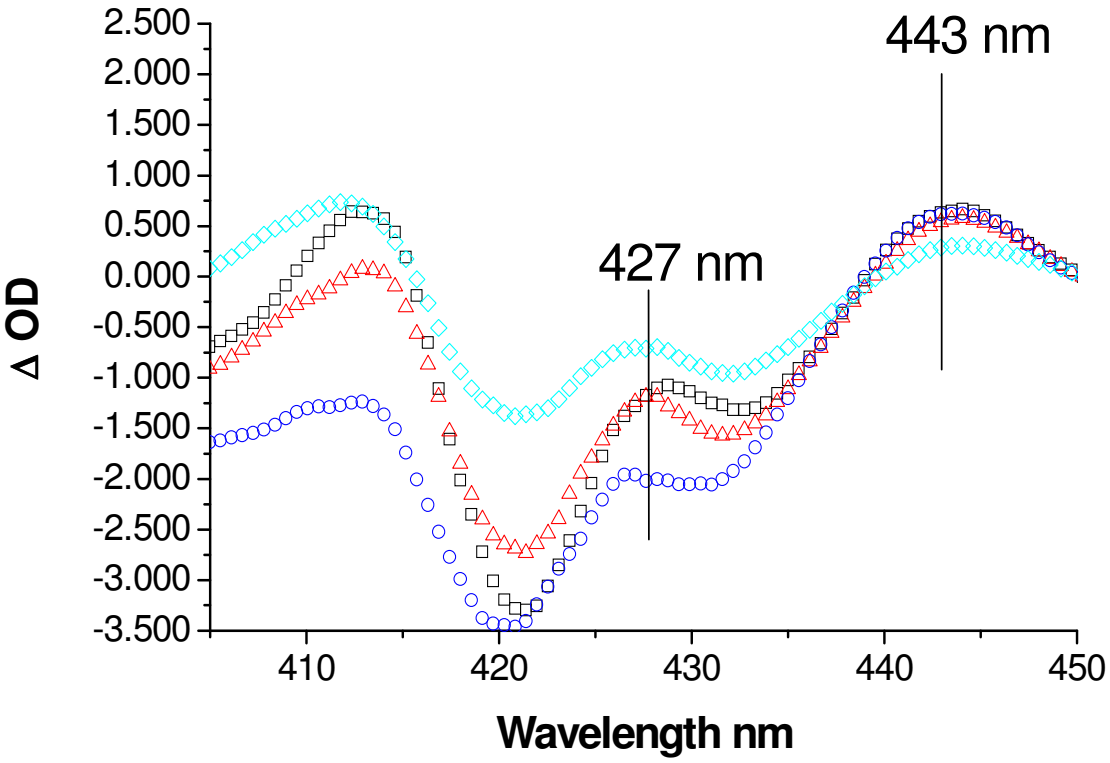

Figure 3.6 Soret band region of 1:500 MbCO and H_2O_2 with CO substracted. Black squares are 120 ns, red triangles 300 ns, blue circles 420 ns and cyan diamonds 540 ns. The spectra resolution was of 0.002 ΔOD.

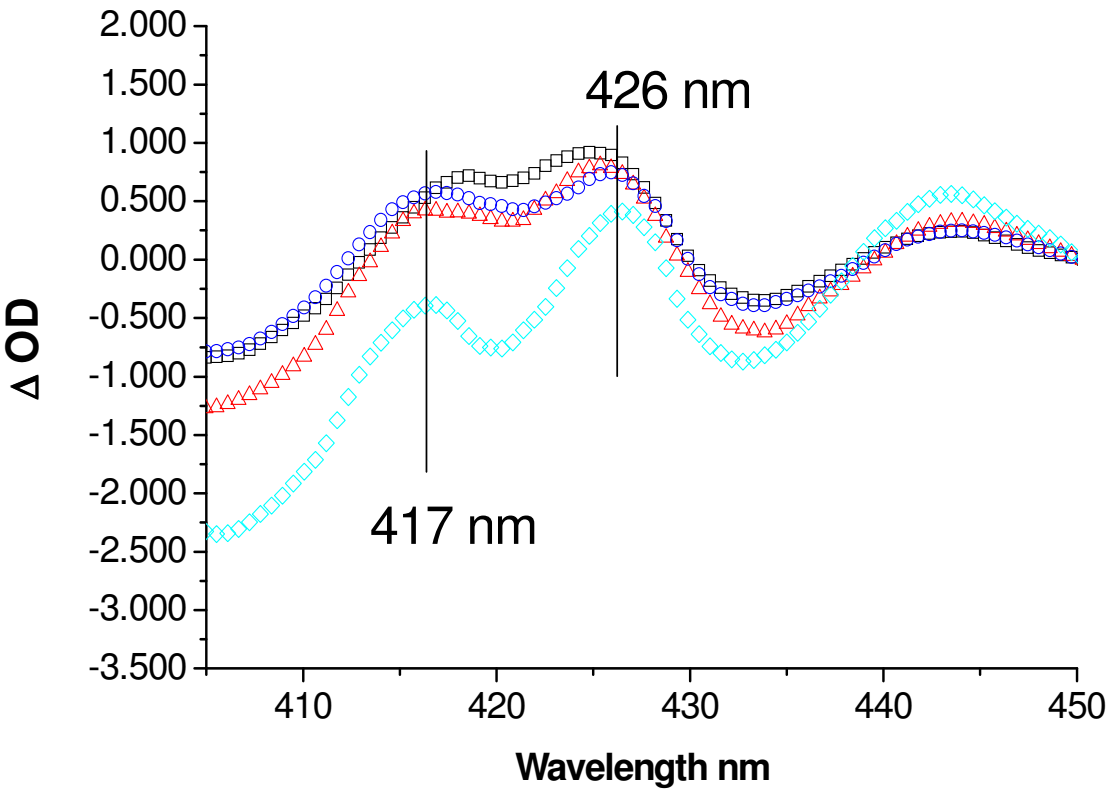

Figure 3.7 Soret band region of 1:1000 MbCO and H_2O_2 with CO substracted. Black squares are 120 ns, red triangles 300 ns, blue circles 420 ns and cyan diamonds 540 ns. The spectra resolution was of 0.002 ΔOD.

results are very significant, since it allowed us to detect the Compound 0 transient species and specify its life time at approximately around 600 ns at low hydrogen peroxide concentration. However, as Figure 3.5 indicated this species lifetime can be shorter than 60 ns at high hydrogen peroxide concentration. Regarding this, Figure 3.8 shows that at 300 ns, the Compound 0 transient increases with increases in the concentration of hydrogen peroxide.

Table 3.1 shows the proposed wavelength and life time of the transient species being discussed upon the reaction between Mb and hydrogen peroxide in the timescales shorter than microseconds. The 426 nm peak it is attributed to Compound 0 or hydroperoxy species.

Table 3-1 Sumary of the spectra bands for the reaction of MbCO with hydrogen peroxide with MbCO subtraction.

Sumary of the reaction of MbCO with H_2O_2				
MbCO/ H_2O_2	**Compound 0 /Hydroperoxy** Soret λ	**Compound I** Soret λ	**Compound II** Soret λ	**Compound 0** Lifetime ns
1:10	**426 nm**	**NA**	**422 nm**	**~ 600 ns**
1:500	**427 nm**	**NA**	**422 nm**	**~ 300 ns**
1:1000	**426 nm**	**NA**	**418 nm**	**< 60 ns**

Because it's similar electronic structure it is impossible to distinguish between both species merely using UV-Vis spectra because of it's near and broad peaks. Figure 3.9 presents the reaction mechanism suggested for describing the behavior of the 426 nm band transition decay towards 418 nm band.

The MbCO photolysis by the laser flash is followed by the reaction between deoxyMb and H_2O_2. This heme Fe(II) species coordinates with H_2O_2 producing the heme ferric hydroperoxide complex. This is followed by a proton that is abstracted from this

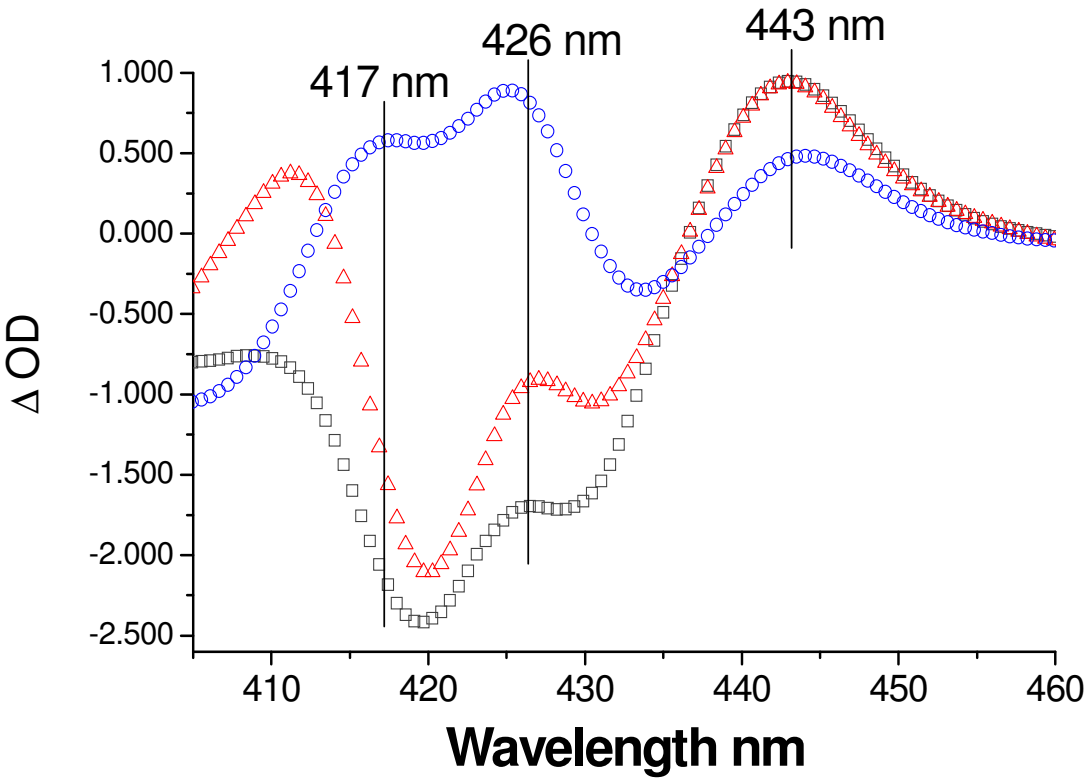

Figure 3.8 Soret band region of MbCO and H_2O_2 with CO substracted at 300 ns. Squares are 1:10 concetration ratio, triangles 1:500 and circles 1:1000. The spectra resolution was of 0.002 ΔOD.

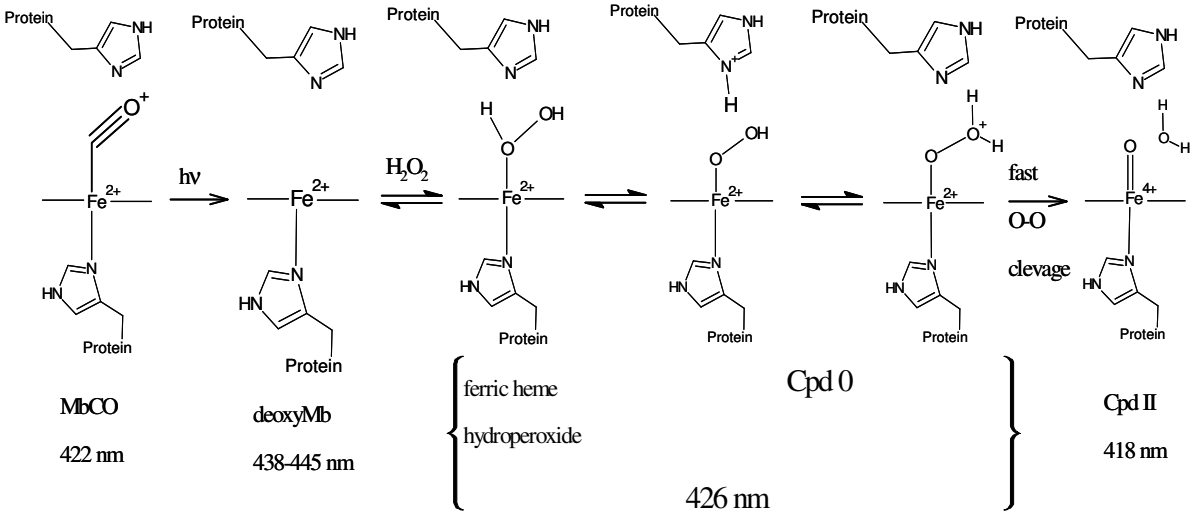

Figure 3.9 Proposed reaction mechanism of MbCO with hydrogen peroxide.

complex by the histidine E7 producing the Compound 0 intermediate species. Thus, the HisE7 is helping in the migration of the proton from the oxygen coordinated to the iron to next oxygen. This consequently gives rise to water and the ferryl Compound II species because of the O-O bond cleavage. This mechanism is also supported by data observed in other heme systems, for example, X-ray diffraction of chloroperoxidase shows a proximal Fe-O distance of 1.9 Å for Compound 0 (Kühnel et al., 2007). Also, theoretical calculations experiments for HRP show that, as expected, Compound 0 has a doublet spin ground state with a Fe-O distance of 1.969 Å in accordance with reported X-ray data. The Compound 0 species itself is generated after deprotonation of the proximal OH of H_2O_2 by the His42 residue. Subsequently, the OH^- group of Compound 0 is pulled by Arg38 and gets reprotonated by His42(H^+) to form a water molecule and Compound I species (Derat and Shaik, 2006). Molecular Dynamics simulations with Perturbed Matrix Method bond calculation (Zazza et al., 2008) showed the thermodynamics of hydroperoxide proton transfer for the formation of Compound 0 in HRP enzyme. This reaction can be described essentially as a stepwise process in which, first, there is a proton transfer from the heme ferric hydroperoxide species to the His 42 giving rise to the Compound O species, and second, a transfer of this proton from the His residue to the distal oxygen of the Compound O species promoting the heterolytical cleavage of the O-O bond (Zazza et al., 2008). Also, Compound 0 is the species mainly postulated to participate in the styrene epoxidation by cytochrome P450 instead of Compound I as previously believed (Matsumura et al., 2008).

4. CONCLUSIONS AND FUTURE WORK

Therefore, all the evidence presented here clearly suggest that for the fist time the 426 nm species has been observed at room temperature in the reaction between Mb and hydrogen peroxide, can be assigned as the transient Compound O derivatives, i.e. Fe^{3+}-HOOH and/or Fe^{3+}-OOH species. The data also allows suggesting a model were hydrogen peroxide binds to deoxy species and forms the hydroperoxide species and later Compound 0. After the proton migration the O-O cleavage takes place and it give rise to the Compound II species which was presented in the reaction scheme in Figure 3.9. Furthermore, it is postulated that the distal His amino acid in the E7 position play a critical role in the proton shift from the proximal oxygen ligated to the iron to the distal one which later helps in the O-O cleavage. All these results support the Poulos-Kraut mechanism. The data also provided evidence at room temperature of the existence of Compound O precursor of Compound II as function of deoxy heme Fe(II) derivative. Future work should include determining the vibrational spectra of the transient species at 424 nm and 422 nm respectively. This can be accomplished by coupling a stopped flow system to a time resolved Resonance Raman spectroscopy system, and follow the reaction between Mb and hydrogen peroxide as function of time.

5. REFERENCES

1. Antonini E, Wyman J, Bucci E, Fronticelli C, Brunori M, Reichlin M & Fanelli A (1965) The oxygen equilibrium of the hybrids of canine and human haemoglobin. *Biochim Biophys Acta* **104**, 160-6.
2. Bursell S & King GL (2000) The Potential Use of Glutathionyl Hemoglobin as a Clinical Marker of Oxidative Stress. *Clin. Chem.* **46**, 145-146.
3. Carlsson GH, Nicholls P, Svistunenko D, Berglund GI & Hajdu J (2005) Complexes of horseradish peroxidase with formate, acetate, and carbon monoxide. *Biochemistry* **44**, 635-42.
4. Carver T, Rohlfs R, Olson J, Gibson Q, Blackmore R, Springer B & Sligar S (1990) Analysis of the kinetic barriers for ligand binding to sperm whale myoglobin using site-directed mutagenesis and laser photolysis techniques. *J. Biol. Chem.* **265**, 20007-20020.
5. Chatfield M, La Mar G & Kauten R (1987) Proton NMR characterization of isomeric sulfmyoglobins: preparation, interconversion, reactivity patterns, and structural features. *Biochemistry* **26**, 6939-50.
6. Chelikani P, Fita I & Loewen P (2004) Diversity of structures and properties among catalases. *Cellular and Molecular Life Sciences (CMLS)* **61**, 192-208.
7. Cotton FA, Murillo CA & Bochman M *Advance Inorganic Chemistry*, 6th ed. Wiley-Interscience.
8. De Jesus-Bonilla W, Cortes-Figueroa J, Souto-Bachiller F, Rodriguez L & Lopez-Garriga J (2001) Formation of compound I and compound II ferryl species in the reaction of hemoglobin I from Lucina pectinata with hydrogen peroxide. *Arch Biochem Biophys* **390**, 304-8.
9. Derat E & Shaik S (2006) The Poulos-Kraut mechanism of Compound I formation in horseradish peroxidase: a QM/MM study. *J Phys Chem B* **110**, 10526-33.
10. Egawa T, Shimada H & Ishimura Y (2000) Formation of Compound I in the Reaction of Native Myoglobins with Hydrogen Peroxide. *J. Biol. Chem.* **275**, 34858-34866.
11. Egawa T, Yoshioka S, Takahashi S, Hori H, Nagano S, Shimada H, Ishimori K, Morishima I, Suematsu M & Ishimura Y (2003) Kinetic and Spectroscopic Characterization of a Hydroperoxy Compound in the Reaction of Native Myoglobin with Hydrogen Peroxide. *J. Biol. Chem.* **278**, 41597-41606.
12. Evans S & Brayer G (1990) High-resolution study of the three-dimensional structure of horse heart metmyoglobin. *J Mol Biol* **213**, 885-97.
13. Evans S, Sishta B, Mauk A & Brayer G (1994) Three-Dimensional Structure of Cyanomet-Sulfmyoglobin C. *PNAS* **91**, 4723-4726.
14. Hersleth H, Uchida T, Rohr AK, Teschner T, Schunemann V, Kitagawa T, Trautwein AX, Gorbitz CH & Andersson KK (2007) Crystallographic and Spectroscopic Studies of Peroxide-derived Myoglobin Compound II and Occurrence of Protonated FeIV O. *J. Biol. Chem.* **282**, 23372-23386.

15. Johnson E (1970) The reversion to haemoglobin of sulphhaemoglobin and its coordination derivatives. *Biochim Biophys Acta* **207**, 30-40.
16. Kuhnel K, Derat E, Terner J, Shaik S & Schlichting I (2007) Structure and quantum chemical characterization of chloroperoxidase compound 0, a common reaction intermediate of diverse heme enzymes. *PNAS* **104**, 99-104.
17. Levantino M, Cupane A, Zimanyi L & Ormos P (2004) Different relaxations in myoglobin after photolysis. *PNAS* **101**, 14402-14407.
18. Matsumura H, Wakatabi M, Omi S, Ohtaki A, Nakamura N, Yohda M & Ohno H (2008) Modulation of redox potential and alteration in reactivity via the peroxide shunt pathway by mutation of cytochrome P450 around the proximal heme ligand. *Biochemistry* **47**, 4834-42.
19. Ordway GA & Garry DJ (2004) Myoglobin: an essential hemoprotein in striated muscle. *J. Exp. Biol.* **207**, 3441-3446.
20. Poulos T & Kraut J (1980) The stereochemistry of peroxidase catalysis. *J. Biol. Chem.* **255**, 8199-8205.
21. Poulos T, Edwards S, Wariishi H & Gold M (1993) Crystallographic refinement of lignin peroxidase at 2 A. *J. Biol. Chem.* **268**, 4429-4440.
22. Prasad S & Mitra S (2004) Substrate modulates compound I formation in peroxide shunt pathway of Pseudomonas putida cytochrome P450(cam). *Biochem Biophys Res Commun* **314**, 610-4.
23. Rajarathnam K, La Mar GN, Chiu ML, Sligar SG, Singh JP & Smith KM (1991) Proton NMR hyperfine shift pattern as a probe for ligation state in high-spin ferric hemoproteins: water binding in metmyoglobin mutants. *J. Am. Chem. Soc.* **113**, 7886-7892.
24. Rodriguez-Guilbe MM (2005) The Role of Ultrafast Events of Hemoglobin I and Hemoglobin II Ligand
Complexes from Lucina pectinata. , 55-58.
25. Scheler W, Schoffa G & Jung F (1957) Light absorption and paramagnetic susceptibility of the derivatives of horse and Chironomus methemoglobins and of horse metmyoglobin. *Biochem Z* **329**, 232-46.
26. Seib KL, Wu H, Kidd SP, Apicella MA, Jennings MP & McEwan AG (2006) Defenses against Oxidative Stress in Neisseria gonorrhoeae: a System Tailored for a Challenging Environment. *Microbiol. Mol. Biol. Rev.* **70**, 344-361.
27. Shintaku M, Matsuura K, Yoshioka S, Takahashi S, Ishimori K & Morishima I (2005) Absence of a Detectable Intermediate in the Compound I Formation of Horseradish Peroxidase at Ambient Temperature. *J. Biol. Chem.* **280**, 40934-40938.
28. Sugimoto T, Unno M, Shiro Y, Dou Y & Ikeda-Saito M (1998) Myoglobin Mutants Giving the Largest Geminate Yield in CO Rebinding in the Nanosecond Time Domain. *Biophys. J.* **75**, 2188-2194.
29. Tanaka M, Matsuura K, Yoshioka S, Takahashi S, Ishimori K, Hori H & Morishima I (2003) Activation of Hydrogen Peroxide in Horseradish Peroxidase Occurs within ~200 {micro}s Observed by a New Freeze-Quench Device. *Biophys. J.* **84**, 1998-2004.
30. van Dalen C & Kettle A (2001) Substrates and products of eosinophil peroxidase. *Biochem. J.* **358**, 233-9.